University of Wisconsin - Madison

MADPH-95-907
September 1995

S to P wave form factors in semileptonic B decays

Siniša Veseli and M.G. Olsson

Department of Physics, University of Wisconsin, Madison, WI 53706

Abstract

We apply HQET to semileptonic B and B_s meson decays into the observed charmed P wave states. In order to examine the sensitivity of the results to the choice of a specific model, we perform all calculations using several different meson models, and find that uncertainty introduced by the choice of a particular model is about 30%. Specifically, assuming $\tau_B = 1.50ps$ and $V_{cb} = 0.040$, we obtain branching ratios of $(0.27 \pm 0.08)\%$ and $(0.45 \pm 0.14)\%$ for $B \to D_1 l \bar{\nu}_l$ and $B \to D_2^* l \bar{\nu}_l$ decays, respectively.

1 Introduction

As more B mesons are produced at major accelerators it has become imperative to gain understanding of how they decay. If the final hadron state consists of a meson containing a heavy quark, heavy quark symmetry [1] and heavy quark effective theory (HQET) [2, 3] provide a powerful assistance.

Since an infinitely massive heavy quark does not recoil from the emission or absorption of soft ($E \approx \Lambda_{QCD}$) gluons, and since magnetic interactions of such a quark are negligible ($\sim \frac{1}{m_Q}$), the strong interactions of the heavy quark are independent of its mass and spin, and the total angular momentum j of the LDF is a good quantum number. Because of this, HQET leads to relations between different form factors describing transitions in which a hadron containing a heavy quark Q and moving with four-velocity v^μ, decays into another hadron containing a heavy quark Q', and moving with four-velocity v'^μ. In this way the number of independent form factors for these decays is significantly reduced.

Semileptonic decays into hadrons account for over 20% of all B decays. In the case of B^- meson decaying into electron, neutrino, and all hadrons the branching ratio is [4]

$$BR(B^- \to Xe^-\bar{\nu}) = (10.49 \pm 0.46)\% \ . \tag{1}$$

Most of the inclusive rate is accounted for by $X = D$ and $X = D^*(2010)$. The measured branching ratios for these final states are [5]

$$BR(B^- \to D^*e^-\bar{\nu}) = (5.13 \pm 0.84)\% \ , \tag{2}$$

$$BR(B^- \to De^-\bar{\nu}) = (1.95 \pm 0.55)\% \ . \tag{3}$$

This leaves $(3.4 \pm 1.1)\%$ of the hadrons unaccounted for.

In this paper we investigate B decays into the P wave D meson states $D_1(2420)$ and $D_2^*(2460)$, for which some experimental data is becoming available, and also the corresponding B_s decays. We use the covariant trace formalism [6, 7, 8] and

HQET to obtain expressions for branching ratios in terms of the non-perturbative Isgur-Wise (IW) form factors. In order to calculate these form factors we employ expressions (consistent with the trace formalism), in terms of the light degrees of freedom (LDF) wave functions and energies [9]. By performing all calculations using four different models and two different one basis state estimates, we also examine sensitivity of our results to the choice of a specific model.

In Sections 2, 3 and 4 we review the covariant representation of states, decay rates for $B \to D_X l \bar{\nu}_l$, and the calculation of IW functions, respectively. In Section 5 we discuss the four heavy-light models which are employed in this paper. We also discuss estimates which use only one basis state as the wave function of the LDF. The model dependence of our results will be judged by the range of prediction of these calculations. Our main results for the S to P wave semileptonic branching ratios for B decay into D_1 and D_2^* (and corresponding B_s decays), are given in Section 6. Our conclusions and a comparison with experiment are summarized in Section 7.

2 Covariant representation of states

The covariant trace formalism, formulated in [6, 7] and generalized to excited states in [8], is most convenient for counting of the number of independent form factors. Following [8], and using the notation of [10], the lowest lying mesonic states with mass m and four velocity v can be described as follows:

$$C(v) = \frac{1}{2}\sqrt{m}(\not{v}+1)\gamma_5 \,, \qquad J^P = 0^- \,,\ j = \frac{1}{2} \,, \tag{4}$$

$$C^*(v,\epsilon) = \frac{1}{2}\sqrt{m}(\not{v}+1)\ \not{\epsilon} \,, \qquad J^P = 1^- \,,\ j = \frac{1}{2} \,, \tag{5}$$

$$E(v) = \frac{1}{2}\sqrt{m}(\not{v}+1) \,, \qquad J^P = 0^+ \,,\ j = \frac{1}{2} \,, \tag{6}$$

$$E^*(v,\epsilon) = \frac{1}{2}\sqrt{m}(\not{v}+1)\gamma_5\ \not{\epsilon} \,, \qquad J^P = 1^+ \,,\ j = \frac{1}{2} \,, \tag{7}$$

$$
\begin{aligned}
F(v,\epsilon) &= \frac{1}{2}\sqrt{m}\sqrt{\frac{3}{2}}(\not{v}+1)\gamma_5[\epsilon^\mu - \frac{1}{3}\not{\epsilon}(\gamma^\mu - v^\mu)] \ , \quad J^P = 1^+ \ , \ j = \frac{3}{2} \ , && (8)\\
F^*(v,\epsilon) &= \frac{1}{2}\sqrt{m}(\not{v}+1)\gamma_\nu\epsilon^{\mu\nu} \ , \qquad J^P = 2^+ \ , \ j = \frac{3}{2} \ , && (9)\\
G(v,\epsilon) &= \frac{1}{2}\sqrt{m}\sqrt{\frac{3}{2}}(\not{v}+1)[\epsilon^\mu - \frac{1}{3}\not{\epsilon}(\gamma^\mu + v^\mu)] \ , \quad J^P = 1^- \ , \ j = \frac{3}{2} \ , && (10)\\
G^*(v,\epsilon) &= \frac{1}{2}\sqrt{m}(\not{v}+1)\gamma_5\gamma_\nu\epsilon^{\mu\nu} \ , \qquad J^P = 2^- \ , \ j = \frac{3}{2} \ . && (11)
\end{aligned}
$$

In these expressions ϵ^μ is the polarization vector for spin 1 states (satisfying $\epsilon\cdot v = 0$), while the tensor $\epsilon^{\mu\nu}$ describes a spin 2 object ($\epsilon^{\mu\nu} = \epsilon^{\nu\mu}$, $\epsilon^{\mu\nu}v_\nu = 0$, $\epsilon^\mu{}_\mu = 0$). For each j there are two degenerate heavy meson states ($J = j \pm \frac{1}{2}$) forming a spin symmetry doublet: (C, C^*) is the $L = 0$ doublet, (E, E^*) and (F, F^*) are the two $L = 1$ doublets, and (G, G^*) is an $L = 2$ doublet.

In the covariant trace formalism matrix elements of bilinear currents of two heavy quarks ($J(q) = \bar{Q}'\Gamma Q$) between the physical meson states are calculated by taking the trace ($\omega = v \cdot v'$),

$$
\langle\Psi'(v')|J(q)|\Psi(v)\rangle = \mathrm{Tr}[\bar{M}'(v')\Gamma M(v)]\mathcal{M}_l(\omega) \ , \tag{12}
$$

where M' and M denote appropriate matrices from (4)-(11), $\bar{M} = \gamma^0 M^\dagger \gamma^0$, and $\mathcal{M}_l(\omega)$ represents the LDF. Again following [8, 10], we define the IW functions for the transitions of a 0^- ground state into an excited state by

$$
\mathcal{M}_l(\omega) = \begin{cases} \xi_C(\omega) \ , & C \to (C, C^*) \ , \\ \xi_E(\omega) \ , & C \to (E, E^*) \ , \\ \xi_F(\omega)v_\mu \ , & C \to (F, F^*) \ , \\ \xi_G(\omega)v_\mu \ , & C \to (G, G^*) \ . \end{cases} \tag{13}
$$

The vector index in the last two definitions will be contracted with the one in the representations of excited states (8)-(11).

3 Decays $B \to D_X l \bar{\nu}_l$ in the heavy quark limit

Denoting the four-velocities of B and D_X mesons as v^μ and v'^μ, respectively, and assuming that lepton masses are zero, the momentum transfer is given by ($\omega = v \cdot v'$)

$$q^2 = (m_B v - m_{D_X} v')^2 = (p_1 + p_2)^2 = m_B^2 + m_{D_X}^2 - 2 m_B m_{D_X} \omega \ . \tag{14}$$

Using (14), and denoting

$$x = (p_1 + m_{D_X} v')^2 = (m_B v - p_2)^2 \ , \tag{15}$$

the standard expression [11] for the width of the semileptonic decay of a B meson into any of the charmed meson states D_X can be written as

$$\frac{d\Gamma}{d\omega} = \frac{m_{D_X}}{128 \pi^3 m_B^2} \int_{x_-}^{x_+} dx \overline{|\mathcal{M}|^2} \ , \tag{16}$$

where $x_\pm = m_B m_{D_X} (\omega \pm \sqrt{\omega^2 - 1})$. The invariant amplitude $\mathcal{M}$,

$$\mathcal{M} = \frac{G_F V_{cb}}{\sqrt{2}} \bar{u}_l \gamma^\mu (1 - \gamma^5) v_{\bar{\nu}} \langle D_X(v', \epsilon') | \bar{c} \gamma_\mu (1 - \gamma^5) b | B(v) \rangle \ , \tag{17}$$

after squaring and summing over l and $\bar{\nu}_l$ spins and D_X polarization, yields

$$\overline{|\mathcal{M}|^2} = \frac{1}{2} G_F^2 |V_{cb}|^2 L_{\mu\nu} H^{\mu\nu} \ . \tag{18}$$

Here,

$$L^{\mu\nu} = 8 (p_1^\mu p_2^\nu - g^{\mu\nu} p_1 \cdot p_2 + p_1^\nu p_2^\mu + i \varepsilon^{\mu\nu\alpha\beta} p_{1\alpha} p_{2\beta}) \ , \tag{19}$$

$$H^{\mu\nu} = \sum_{pol} \langle D_X(v', \epsilon') | \bar{c} \gamma^\mu (1 - \gamma^5) b | B(v) \rangle \langle D_X(v', \epsilon') | \bar{c} \gamma^\nu (1 - \gamma^5) b | B(v) \rangle^\dagger \ . \tag{20}$$

The matrix elements needed in $H^{\mu\nu}$ are calculated from (12) using (4)-(11), while the sum over D_X polarization states is performed using standard expressions for spin-1

and spin-2 particles,

$$
\begin{aligned}
M^{(1)}_{\mu\nu}(v) &\equiv \sum_{pol} \epsilon^*_\mu \epsilon_\nu \\
&= -g_{\mu\nu} + v_\mu v_\nu \ , \qquad (21) \\
M^{(2)}_{\mu\nu,\rho\sigma}(v) &\equiv \sum_{pol} \epsilon^*_{\mu\nu} \epsilon_{\rho\sigma} \\
&= \frac{1}{2} M^{(1)}_{\mu\rho}(v) M^{(1)}_{\nu\sigma}(v) + \frac{1}{2} M^{(1)}_{\mu\sigma}(v) M^{(1)}_{\nu\rho}(v) - \frac{1}{3} M^{(1)}_{\mu\nu}(v) M^{(1)}_{\rho\sigma}(v) \ . \qquad (22)
\end{aligned}
$$

Using kinematical identities coming from definitions (14) and (15), and from momentum conservation, we can express $\overline{|\mathcal{M}|^2}$ in terms of ω and x. Performing a simple integration in (16), we find

$$
\frac{d\Gamma_X}{d\omega} = \frac{G_F^2 |V_{cb}|^2}{48\pi^3} m_B^2 m_{D_X}^3 \sqrt{\omega^2 - 1} |\xi_X(\omega)|^2 f_X(\omega, r_X) \ , \qquad (23)
$$

where $r_X = m_{D_X}/m_B$, and the function f_X is given by

$$
\begin{aligned}
f_C(\omega, r_C) &= (\omega^2 - 1)(1 + r_C)^2 \ , \qquad (24) \\
f_{C^*}(\omega, r_{C^*}) &= (\omega + 1)[(\omega + 1)(1 - r_{C^*})^2 + 4\omega(1 - 2\omega r_{C^*} + r_{C^*}^2)] \ , \qquad (25) \\
f_E(\omega, r_E) &= (\omega^2 - 1)(1 - r_E)^2 \ , \qquad (26) \\
f_{E^*}(\omega, r_{E^*}) &= (\omega - 1)[(\omega - 1)(1 + r_{E^*})^2 + 4\omega(1 - 2\omega r_{E^*} + r_{E^*}^2)] \ , \qquad (27) \\
f_F(\omega, r_F) &= \frac{2}{3}(\omega - 1)(\omega + 1)^2[(\omega - 1)(1 + r_F)^2 + \omega(1 - 2\omega r_F + r_F^2)] \ , \qquad (28) \\
f_{F^*}(\omega, r_{F^*}) &= \frac{2}{3}(\omega - 1)(\omega + 1)^2[(\omega + 1)(1 - r_{F^*})^2 + 3\omega(1 - 2\omega r_{F^*} + r_{F^*}^2)] \ , \qquad (29) \\
f_G(\omega, r_G) &= \frac{2}{3}(\omega - 1)^2(\omega + 1)[(\omega + 1)(1 - r_G)^2 + \omega(1 - 2\omega r_G + r_G^2)] \ , \qquad (30) \\
f_{G^*}(\omega, r_{G^*}) &= \frac{2}{3}(\omega - 1)^2(\omega + 1)[(\omega - 1)(1 + r_{G^*})^2 + 3\omega(1 - 2\omega r_{G^*} + r_{G^*}^2)] \ . \qquad (31)
\end{aligned}
$$

Some, but not all of the above expressions can be found in earlier work [12]-[14].

4 IW functions

The only factor in (23) which cannot be calculated from first principles is the IW function for a particular decay. In order to estimate these form factors one has to rely on some model of strong interactions. In the original calculation of radiative rare B decays [10] the IW functions (13) were defined as the overlap between wave functions describing the LDF in the initial and the final mesons (AOM). These authors have chosen the wave functions to be eigenfunctions of orbital angular momentum L (α denotes all other quantum numbers),

$$\Phi_{\alpha L m_L}(\mathbf{x}) = R_{\alpha L}(r) Y_{L m_L}(\Omega) \ , \tag{32}$$

and the form factors were given by (putting a tilde to avoid confusion with our definitions),

$$\begin{aligned} \tilde{\xi}_C(\omega) &= \langle j_0(\tilde{a}r)\rangle_{00} \ , & (33)\\ \tilde{\xi}_E(\omega) &= \sqrt{3}\langle j_1(\tilde{a}r)\rangle_{10} \ , & (34)\\ \tilde{\xi}_F(\omega) &= \sqrt{3}\langle j_1(\tilde{a}r)\rangle_{10} \ , & (35)\\ \tilde{\xi}_G(\omega) &= \sqrt{5}\langle j_2(\tilde{a}r)\rangle_{20} \ . & (36) \end{aligned}$$

In the above

$$\tilde{a} = \tilde{E}'_{\bar{q}}\sqrt{\omega^2 - 1} \ , \tag{37}$$

where $\tilde{E}'_{\bar{q}} = \frac{M' m_{\bar{q}}}{m_{Q'} + m_{\bar{q}}}$ denotes the "inertia parameter" of the LDF in the final heavy meson (with mass M' and heavy quark Q'). The expectation values in (33)-(36) are defined by

$$\langle F(r)\rangle^{\alpha'\alpha}_{L'L} = \int r^2 dr R^*_{\alpha' L'}(r) R_{\alpha L}(r) F(r) \ . \tag{38}$$

To calculate the above overlap integrals, in [10] the radial wave functions of the ISGW model [15] were used. The same approach was followed in [14] for the calculation of semileptonic B meson decays into higher charmed resonances. However, by

comparing the covariant trace formalism of [6, 7, 8] with the wave function approach of [16], it has been recently shown [9] that form factor definitions as pure overlap integrals (used in [10, 14]), are not consistent with the trace formalism.

Under the assumption that heavy mesons can be described using simple non-relativistic (or semi-relativistic) quark model, the rest frame LDF wave functions (with angular momentum j and its projection λ_j), can be written as

$$\phi^{(\alpha L)}_{j\lambda_j}(\mathbf{x}) = \sum_{m_L, m_s} R_{\alpha L}(r) Y_{Lm_L}(\Omega) \chi_{m_s} \langle L, m_L; \frac{1}{2}, m_s | j, \lambda_j; L, \frac{1}{2} \rangle \ , \tag{39}$$

where χ_{m_s} represent the rest frame spinors normalized to one, $\chi^\dagger_{m'_s} \chi_{m_s} = \delta_{m'_s, m_s}$, and α again represents all other quantum numbers. Performing the overlap integrals in the modified Breit frame ($\mathbf{v}' = -\mathbf{v}$) [13], using (39) and form factor definitions consistent with the trace formalism, one can derive [9] expressions for the IW functions, their values, and values of their derivatives at the zero recoil point ($\omega = 1$), in terms of the LDF wave functions. Denoting ($E_{\bar{q}} = M - m_Q$ here refers to the LDF energy of a meson with mass M and heavy quark Q),

$$a = (E_{\bar{q}} + E'_{\bar{q}}) \sqrt{\frac{\omega - 1}{\omega + 1}} \ , \tag{40}$$

and suppressing quantum numbers α' and α, we have:

- $C \to (C, C^*)$ transitions.

$$\xi_C(\omega) = \frac{2}{\omega + 1} \langle j_0(ar) \rangle_{00} \ , \tag{41}$$

$$\xi_C(1) = \langle 1 \rangle_{00} \ , \tag{42}$$

$$\xi'_C(1) = -\frac{1}{2} - \frac{1}{12} (E_{\bar{q}} + E'_{\bar{q}})^2 < r^2 >_{00} \ . \tag{43}$$

- $C \to (E, E^*)$ transitions.

$$\xi_E(\omega) = \frac{2}{\sqrt{\omega^2 - 1}} \langle j_1(ar) \rangle_{10} \ , \tag{44}$$

$$\xi_E(1) = \frac{1}{3}(E_{\bar{q}} + E'_{\bar{q}})\langle r\rangle_{10} \ , \tag{45}$$

$$\xi'_E(1) = -\frac{1}{6}(E_{\bar{q}} + E'_{\bar{q}})\langle r\rangle_{10} - \frac{1}{60}(E_{\bar{q}} + E'_{\bar{q}})^3 < r^3 >_{10} \ . \tag{46}$$

- $C \to (F, F^*)$ transitions.

$$\xi_F(\omega) = \sqrt{\frac{3}{\omega^2 - 1}}\frac{2}{\omega + 1}\langle j_1(ar)\rangle_{10} \ , \tag{47}$$

$$\xi_F(1) = \frac{1}{2\sqrt{3}}(E_{\bar{q}} + E'_{\bar{q}})\langle r\rangle_{10} \ , \tag{48}$$

$$\xi'_F(1) = -\frac{1}{2\sqrt{3}}(E_{\bar{q}} + E'_{\bar{q}})\langle r\rangle_{10} - \frac{1}{40\sqrt{3}}(E_{\bar{q}} + E'_{\bar{q}})^3 < r^3 >_{10} \ . \tag{49}$$

- $C \to (G, G^*)$ transitions.

$$\xi_G(\omega) = \frac{2\sqrt{3}}{\omega^2 - 1}\langle j_2(ar)\rangle_{20} \ , \tag{50}$$

$$\xi_G(1) = \frac{1}{10\sqrt{3}}(E_{\bar{q}} + E'_{\bar{q}})^2\langle r^2\rangle_{20} \ , \tag{51}$$

$$\xi'_G(1) = -\frac{1}{10\sqrt{3}}(E_{\bar{q}} + E'_{\bar{q}})^2\langle r^2\rangle_{20} - \frac{1}{280\sqrt{3}}(E_{\bar{q}} + E'_{\bar{q}})^4 < r^4 >_{20} \ . \tag{52}$$

Note that these expressions include transitions from the ground state into radially excited states. If the two $j = \frac{1}{2}$ states are the same, $E'_{\bar{q}} = E_{\bar{q}}$ and $\xi_C(1)$ is normalized to one. Also note that from (44) and (47) it follows that the two P wave form factors satisfy

$$\xi_E(\omega) = \frac{\omega + 1}{\sqrt{3}}\xi_F(\omega) \ , \tag{53}$$

and in particular

$$\xi_E(1) = \frac{2}{\sqrt{3}}\xi_F(1) \ . \tag{54}$$

It can be also shown [9] that the above formulae can be generalized to any model involving the Dirac equation with a spherically symmetric potential. There, the wave

function has the form

$$\phi^{(\alpha k)}_{j\lambda_j}(\mathbf{x}) = \begin{pmatrix} f^k_{\alpha j}(r)\mathcal{Y}^k_{j\lambda_j}(\Omega) \\ ig^k_{\alpha j}(r)\mathcal{Y}^{-k}_{j\lambda_j}(\Omega) \end{pmatrix} , \tag{55}$$

where $\mathcal{Y}^k_{j\lambda_j}$ are the usual spherical spinors, $k = l$ $(l = j+\frac{1}{2})$ or $k = -l-1$ $(l = j-\frac{1}{2})$, and α again denotes all other quantum numbers. Using (55) one finds that all the expressions (41)-(52) remain unchanged, except for the expectation value (38) which is replaced by

$$\langle F(r)\rangle^{\alpha'\alpha}_{L'L} \to \langle F(r)\rangle^{\alpha'\alpha}_{j'j} = \int r^2 dr[f^{*k'}_{\alpha' j'}(r) f^k_{\alpha j}(r) + g^{*k'}_{\alpha' j'}(r) g^k_{\alpha j}(r)]F(r) \ . \tag{56}$$

Of course, in models with the Dirac equation the two P wave doublets are not degenerate any more ($E'_{\bar{q}} \neq E_{\bar{q}}$), so that relations (53) and (54) are no longer valid.

5 Heavy-light models

Although we have presented here a formalism applicable for a variety of transitions $C \to C, \ldots, G^*$, we shall focus for the rest of the paper on the P wave transitions $B \to D_1 l\bar{\nu}_l$ and $B \to D^*_2 l\bar{\nu}_l$, and their B_s counterparts. The observed D_1 and D^*_2 (or D_{s1} and D^*_{s2}) states are expected to be members of the $j = \frac{3}{2}$ P wave doublet (F, F^*), since $j = \frac{1}{2}$ P wave doublet (E, E^*) will have S wave decays, and therefore these states should be broad resonances and correspondingly much harder to observe. In order to examine the sensitivity of our form factor predictions to the choice of a specific model and its parameters, we have performed calculations of ξ_F using four different models in the heavy-quark limit: ISGW model, semi-relativistic quark model (SRQM), Dirac equation with scalar confinement (DESC), and Salpeter equation with vector confinement (SEVC). For the ISGW model we have used the original parameters from [15]. For the other three models, we have fixed the string tension b in order to reproduce the expected linear Regge behavior, and (for a given

light quark mass $m_{u,d}$), varied the other parameters until a good description of the observed heavy-light mesons was obtained. It turns out that our results are not sensitive to the exact value of the light quark mass. By varying $m_{u,d}$ in the range from 0.300 GeV to 0.350 GeV we have found that specific choice of 0.300 GeV, that we made for the SRQM, DESC and SEVC, does not lead to significant uncertainties, as long as good description of the observed spin-averaged spectrum of heavy-light states is obtained. We have also used a single pseudo-Coulombic (PC) [17] or harmonic oscillator (HO) basis wave functions to obtain form factor predictions. In this case the unknown energy of the LDF was estimated from the recent experimental data [5] for $B \to D^{(*)} l \bar{\nu}_l$ decays, and also from the spin-averaged masses of the known heavy-light states.

5.1 ISGW model

Because of its simplicity, the ISGW model [15] is widely used in combination with HQET for calculations of different form factors. It is a non-relativistic quark model based on the Schrödinger equation with the usual Coulomb plus linear potential,

$$V(r) = -\frac{4\alpha_s}{3r} + c + br \ . \tag{57}$$

The Hamiltonian of the LDF is then given by

$$H_{\bar{q}} = \frac{\mathbf{p}^2}{2\mu} + m_{\bar{q}} + V(r) \ , \tag{58}$$

with $\mu = \frac{m_{\bar{q}} m_Q}{m_{\bar{q}} + m_Q}$.

We have used the original parameters from [15],

$$\begin{aligned} m_{u,d} &= 0.33 GeV \ , \\ m_s &= 0.55 GeV \ , \\ m_c &= 1.82 GeV \ , \end{aligned}$$

$$
\begin{aligned}
m_b &= 5.12 GeV \ , \\
\alpha_s &= 0.50 \ , \\
c &= -0.84 GeV \ , \\
b &= 0.18 GeV^2 \ ,
\end{aligned} \tag{59}
$$

to obtain theoretical predictions for the spin-averaged heavy-light B and D meson states. The results are shown in Table 1. Taking into account that the non-relativistic quark model with linear confinement does not yield linear Regge trajectories, this model provides a reasonable description of many of the known heavy-light meson states. Using the LDF wave functions and energies obtained from the parameters given above, we show in Figures 1 and 2 (with full lines) our predictions (obtained from (47)) for the form factor ξ_F in the semileptonic decays $B \to D_1, D_2^*$ and corresponding B_s decays. For comparison we show with dashed lines the corresponding AOM [10, 14] form factors obtained from (35).

5.2 Semi-relativistic quark model (SRQM)

It was observed in [18] from Lattice QCD simulations that the ground state wave function describing the LDF in heavy-light mesons is in remarkably good agreement with the wave function that one gets from the semi-relativistic quark model. In this model the Hamiltonian describing the LDF is

$$
H_{\bar{q}} = \sqrt{\mathbf{p}^2 + m_{\bar{q}}^2} + V(r) \ , \tag{60}
$$

where

$$
V(r) = -\frac{4\alpha_s}{3r} + br \ . \tag{61}
$$

The SRQM yields linear Regge trajectories with slopes of $\alpha'_{HL} = \frac{1}{4b}$. The slope of the Regge trajectories in the heavy-light case is expected to be exactly twice the slope in the light-light case [19, 20], i.e. $\alpha'_{HL} = 2\alpha'_{LL}$. The observed Regge slope for

the light-light states is $\alpha'_{LL} = 0.88\ GeV^{-2}$ [21]. Therefore, in order to obtain the expected Regge behavior, we fix the string tension b to be[1]

$$\begin{aligned} b &= \frac{1}{4\alpha'_{HL}} \\ &= 0.142\ GeV^2\ . \end{aligned} \tag{62}$$

For a given $m_{u,d}$ we vary the other parameters of the model to account for all observed heavy-light B and D meson states. An example of such fit is given in Table 2, with parameters

$$\begin{aligned} m_{u,d} &= 0.300 GeV \quad \text{(fixed)}\ , \\ m_s &= 0.512 GeV\ , \\ m_c &= 1.437 GeV\ , \\ m_b &= 4.774 GeV\ , \\ \alpha_s &= 0.421\ , \\ b &= 0.142 GeV^2 \quad \text{(fixed)}\ . \end{aligned} \tag{63}$$

As one can see, the agreement of theoretical and experimental results is excellent. We show with dotted lines in Figures 3 and 4 the form factors for the decays $B \to D_1, D_2^*$ and $B_s \to D_{s1}, D_{s2}^*$, respectively. From these two figures one can see that form factors for the two decays are almost identical. The near equality of the B and B_s form factors is a reflection of the similarity of the wave functions for mesons with or without a strange quark. This in turns explains the near equality [11] of the $m_{D^*} - m_D \simeq m_{D_s^*} - m_{D_s}$ (or $m_{B^*} - m_B \simeq m_{B_s^*} - m_{B_s}$) hyperfine differences.

[1] Although this method of choosing the effective string tension ensures the correct Regge behavior, it may not correspond to the correct static string tension. If it does not, it indicates the interaction dynamics is incorrect.

5.3 Dirac equation with scalar confinement (DESC)

Scalar confinement is the only type of confinement potential that has correct sign of the spin-orbit coupling. In the Dirac equation it also yields linear Regge trajectories, but with slope of $\alpha'_{HL} = \frac{1}{2b}$, and one can also obtain very good description of the spin averaged heavy-light states [20]. In this model the LDF Hamiltonian is given by

$$H_{\bar{q}} = H_0 + \beta br - \frac{4\alpha_s}{3r} \ , \tag{64}$$

where H_0 is the free particle Dirac Hamiltonian,

$$H_0 = \boldsymbol{\alpha} \cdot \mathbf{p} + \beta m_{\bar{q}} \ . \tag{65}$$

Reduction of (64) to the set of radial equations is standard [22], and the method of solution is described in [20]. In order to have the expected Regge behavior, we fix b to

$$\begin{aligned} b &= \frac{1}{2\alpha'_{HL}} \\ &= 0.284 \ GeV^2 \ , \end{aligned} \tag{66}$$

and, for a given $m_{u,d}$, we vary the other parameters of the model to account for all observed heavy-light B and D meson states. In Table 3 we show an example of such fit, with parameters

$$\begin{aligned} m_{u,d} &= 0.300 GeV \quad \text{(fixed)} \ , \\ m_s &= 0.465 GeV \ , \\ m_c &= 1.357 GeV \ , \\ m_b &= 4.693 GeV \ , \\ \alpha_s &= 0.462 \ , \\ b &= 0.284 GeV^2 \quad \text{(fixed)} \ . \end{aligned} \tag{67}$$

The agreement of theoretical and experimental results is again very good. The form factors for the decays $B \to D_1, D_2^*$ and $B \to D_{s1}, D_{s2}^*$, resulting from the DESC model, with parameters given above, are shown with dashed lines in Figures 3 and 4. Note that form factors obtained from this model are very similar to the ones obtained from SRQM.

5.4 Salpeter equation with vector confinement (SEVC)

The instantaneous version of the Bethe-Salpeter equation [23, 24] (usually referred to as the Salpeter equation [25]) is widely used for the discussion of bound state problems. It is also equivalent [26] to the so called "no-pair" equation [27], which was introduced in order to avoid the problem of mixing of positive and negative energy states that occurred in the Dirac equation for the helium atom. A similar problem also occurs for a single fermionic particle moving in the confining Lorentz vector potential. For a very long time [28] it has been known that there are no normalizable solutions to the Dirac equation in this case.

It has been shown analytically for the heavy-light case [20], and numerically for the case of fermion and antifermion with arbitrary mass [29, 30], that in this type of model linear scalar confinement does not yield linear Regge trajectories. We have therefore used vector confinement, even though it is well known to give the wrong sign of the spin-orbit coupling. In terms of the free particle Dirac Hamiltonian H_0, potential $V(r)$ from (61), and the positive energy projection operator Λ_+ defined as ($E_0 = \sqrt{\mathbf{p}^2 + m_{\bar{q}}^2}$)

$$\Lambda_+ = \frac{E_0 + H_0}{2E_0} \ , \tag{68}$$

the LDF Hamiltonian for the heavy-light Salpeter equation with vector confinement is given by

$$H_{\bar{q}} = H_0 + \Lambda_+ V(r) \Lambda_+ \ . \tag{69}$$

The reduction of (69) to a pair of coupled radial equations, as well as the solution

method, is described in [20]. In Table 4 we show an example of theoretical prediction for the spectrum of spin-averaged heavy-light states. As in the case of SRQM and DESC, the agreement of theory and experiment is excellent. The parameters of the model were

$$\begin{aligned} m_{u,d} &= 0.300 GeV \quad \text{(fixed)} \ , \\ m_s &= 0.598 GeV \ , \\ m_c &= 1.404 GeV \ , \\ m_b &= 4.739 GeV \ , \\ \alpha_s &= 0.534 \ , \\ b &= 0.142 GeV^2 \quad \text{(fixed)} \ . \end{aligned} \tag{70}$$

Here, b was again fixed to 0.142 GeV^2 since the model yields the Regge slope of $\alpha'_{HL} = \frac{1}{4b}$, as in the case of SRQM. We again calculate the form factors resulting from the above parameters. Results for the decays $B \to D_1, D_2^*$ and $B \to D_{s1}, D_{s2}^*$, are shown with full lines in Figures 3 and 4, respectively. Form factors obtained from this model are about 10% larger than the ones obtained from the SRQM and the DESC.

5.5 One basis state estimates

Quite often (as was done in [10, 31]) one finds in the literature estimates for form factors that use a single basis state as a wave function of the LDF. Usually, it is argued on the basis of the original ISGW model [15], that it should be the lowest harmonic oscillator (HO) wave function with the scale parameter around 0.4 GeV. However, on the basis of lattice data [18] one might argue that pseudo-Coulombic (PC) basis states [17] are more suitable for such a purpose. We show in Figure 5 a comparison of the lattice wave function for the heavy-light system calculated in [18], with both PC (full line) and HO $1S$ radial wave function with the scale parameter

$\beta_S = 0.40\ GeV$.

Once we choose the LDF wave function, there are still two unknown parameters ($E_{\bar{q}}$ and $E'_{\bar{q}}$) in the expression (47) needed for the calculation of ξ_F. In [32] the energy of the LDF was estimated by comparing the theoretical prediction for the IW function ξ_C obtained from (41) with the recent experimental data [5] for the exclusive semileptonic $B \to D^{(*)} l \bar{\nu}_l$ decay. It is straightforward to repeat the same analysis using only one basis state, and obtain the range of acceptable values for $E_{\bar{q}}$ in $1S$ state (B, B^* or D, D^* mesons). The corresponding value for the other $1S$ (B_s, B_s^* mesons) or $1P$ (D_1, D_2^* and D_{s1}, D_{s2}^* mesons) doublets is then determined by the difference between the spin averaged masses of the doublet with unknown $E_{\bar{q}}$ and the one where $E_{\bar{q}}$ is known (B, B^* or D, D^* doublets). In the following we present the necessary formulae for this analysis for both PC and HO wave functions.

5.5.1 Pseudo-Coulombic basis states (PC)

The lowest $1S$ and $1P$ wave functions are [17]

$$R_{1S}(r) = 2\beta_S^{3/2} \exp(-\beta_S r) , \tag{71}$$

$$R_{1P}(r) = \frac{2}{\sqrt{3}} \beta_P^{5/2} r \exp(-\beta_P r) . \tag{72}$$

From (41) we find (with $E_{\bar{q}} = E'_{\bar{q}}$)

$$\xi_C(\omega) = \frac{2\beta_S^4(\omega+1)}{((\omega+1)\beta_S^2 + (\omega-1)E_{\bar{q}}^2))^2} . \tag{73}$$

Using this expression for ξ_C with $\beta_S = 0.40\ GeV$ (the corresponding wave function is shown with full line in Figure 5), and performing the analysis as described in [32], we find that the lowest χ^2 of 0.372 per degree of freedom is obtained for

$$E_{\bar{q}} = 0.320\ GeV , \tag{74}$$

for the (B, B^*) and (D, D^*) doublets. Adding spin-averaged mass differences given in Tables 1-4 we find

$$E_{\bar{q}} = 0.415\ GeV\ , \tag{75}$$

$$E_{\bar{q}} = 0.792\ GeV\ , \tag{76}$$

$$E_{\bar{q}} = 0.905\ GeV\ , \tag{77}$$

for the (B_s, B_s^*), (D_1, D_2^*), and (D_{s1}, D_{s2}^*) doublets, respectively. Using these values for $E_{\bar{q}}$, and assuming $\beta_P = \beta_S = 0.40\ GeV$ in the expressions valid for $C \to F, F^*$ transitions,

$$\xi_F(\omega) = 64 \frac{\beta_P^{5/2}\beta_S^{3/2}(\beta_S+\beta_P)(E_{\bar{q}}+E'_{\bar{q}})(\omega+1)}{((\omega+1)(\beta_S+\beta_P)^2+(\omega-1)(E_{\bar{q}}+E'_{\bar{q}})^2)^3}\ , \tag{78}$$

$$\xi_F(1) = 16 \frac{\beta_P^{5/2}\beta_S^{3/2}}{(\beta_S+\beta_P)^5}(E_{\bar{q}}+E'_{\bar{q}})\ , \tag{79}$$

$$\xi'_F(1) = -16 \frac{\beta_P^{5/2}\beta_S^{3/2}}{(\beta_S+\beta_P)^5}(E_{\bar{q}}+E'_{\bar{q}})\left[1+\frac{3}{2}\frac{(E_{\bar{q}}+E'_{\bar{q}})^2}{(\beta_S+\beta_P)^2}\right]\ , \tag{80}$$

we calculate form factors for $B \to D_1, D_2^*$ and $B_s \to D_{s1}, D_{s2}^*$ decays, shown with the full lines in Figures 6 and 7, respectively.

5.5.2 Harmonic oscillator basis states (HO)

Here, the lowest $1S$ and $1P$ states,

$$R_{1S}(r) = \frac{2\beta_S^{3/2}}{\pi^{1/4}} \exp\left(-\beta_S^2 r^2/2\right)\ , \tag{81}$$

$$R_{1P}(r) = \sqrt{\frac{8}{3}}\frac{\beta_P^{5/2}}{\pi^{1/4}} r \exp\left(-\beta_P^2 r^2/2\right)\ , \tag{82}$$

used in (41) give (with $E_{\bar{q}} = E'_{\bar{q}}$)

$$\xi_C(\omega) = \frac{2}{\omega+1}\exp\left[-\frac{E_S^2(\omega-1)}{\beta_S^2(\omega+1)}\right]\ . \tag{83}$$

Again, using this expression for ξ_C with $\beta_S = 0.40\ GeV$, and performing the analysis from [32], we find that

$$E_{\bar{q}} = 0.444\ GeV\ , \tag{84}$$

(for the (B, B^*) and (D, D^*) doublets), yields the lowest χ^2 of 0.357 per degree of freedom (the corresponding wave function is shown with the dashed line in Figure 5). This implies

$$E_{\bar{q}} = 0.539\ GeV\ , \tag{85}$$

$$E_{\bar{q}} = 0.916\ GeV\ , \tag{86}$$

$$E_{\bar{q}} = 1.029\ GeV\ , \tag{87}$$

for the (B_s, B_s^*), (D_1, D_2^*), and (D_{s1}, D_{s2}^*) doublets, respectively. The harmonic oscillator expressions valid for $C \to F, F^*$ transitions are

$$\xi_F(\omega) = 8\frac{\beta_P^{5/2}\beta_S^{3/2}}{(\beta_S^2+\beta_P^2)^{5/2}}(E_{\bar{q}}+E'_{\bar{q}})\frac{1}{(\omega+1)^2}\exp\left[-\frac{(E_{\bar{q}}+E'_{\bar{q}})^2(\omega-1)}{2(\beta_S^2+\beta_P^2)(\omega+1)}\right]\ , \tag{88}$$

$$\xi_F(1) = 2\frac{\beta_P^{5/2}\beta_S^{3/2}}{(\beta_S^2+\beta_P^2)^{5/2}}(E_{\bar{q}}+E'_{\bar{q}})\ , \tag{89}$$

$$\xi'_F(1) = -2\frac{\beta_P^{5/2}\beta_S^{3/2}}{(\beta_S^2+\beta_P^2)^{5/2}}(E_{\bar{q}}+E'_{\bar{q}})\left[1+\frac{1}{4}\frac{(E_{\bar{q}}+E'_{\bar{q}})^2}{(\beta_S^2+\beta_P^2)}\right]\ . \tag{90}$$

These formulae, with $\beta_P = \beta_S = 0.40\ GeV$ and $E_{\bar{q}}$ values given above, yield form factors shown with the dashed lines in Figures 6 and 7 for $B \to D_1, D_2^*$ and $B_s \to D_{s1}, D_{s2}^*$ decays, respectively.

6 Results for the decay rates and branching ratios

For calculation of the decay rates we have chosen $V_{cb} = 0.040$ as the reference value. Also, we have used [11] $\tau_B^{ref} = 1.50 \times 10^{-12} s$ (for $B \to D_1, D_2^*$ decays), and $\tau_{B_s}^{ref} = 1.34 \times 10^{-12} s$ (for $B_s \to D_{s1}, D_{s2}^*$ decays). In order to examine sensitivity of form

factors to the choice of parameters of a specific model, we have fixed m_c between 1.2 GeV and 1.6 GeV, and varied other parameters of SRQM, DESC, and SEVC, until a good description of the spin-averaged spectra is obtained. For the one basis state estimates we have performed the analysis from [32] and obtained ranges of acceptable $E_{\bar{q}}$ values ((B, B^*) and (D, D^*) doublets) for each β_S in the range from 0.3 GeV to 0.5 GeV. For example, for $\beta_S = 0.3$ GeV we found that $E_{\bar{q}}$ for (B, B^*) and (D, D^*) doublets ranges from 0.208 GeV to 0.271 GeV in the PC case, while the corresponding range in the HO case was 0.288 GeV to 0.374 GeV. Similarly, for $\beta_S = 0.5$ GeV the results were 0.346 GeV to 0.451 GeV in the PC case, and 0.480 GeV to 0.623 GeV in the HO case. By adding the appropriate spin-averaged mass differences we obtained values of $E_{\bar{q}}$ for the other doublets. Assuming $\beta_P = \beta_S$, and varying β_S in the range from 0.3 GeV to 0.5 GeV (and $E_{\bar{q}}$ in the range corresponding to a given β_S), we obtained the acceptable ranges for all decay rates and branching ratios considered in this paper.

All results obtained from different models and one basis state estimates (for $\xi_F(1)$, $\xi'_F(1)$, decay rates and branching ratios), are collected in Tables 5-8. As one can see, the uncertainty introduced by the choice of parameters within a specific model is the largest for the SRQM (about 30%), and the smallest for the estimates which use pseudo-Coulombic basis states (only about 5%). For other models the uncertainty is about (15-25)%. We also note that the HO wave function estimates (which are the most commonly encountered in the literature) yield branching ratios that are significantly larger than those obtained from the more realistic models, for all decays considered in this paper.

From the three models SRQM, DESC and SEVC, which successfully account for the known heavy-light masses, we obtain the following ranges for the S to P wave decay rates:

$$\Gamma(B \to D_1 l \bar{\nu}_l) \;=\; (1.16 \pm 0.38) \times \left|\frac{V_{cb}}{0.040}\right|^2 10^{-15} GeV \;, \tag{91}$$

$$\Gamma(B \to D_2^* l\bar{\nu}_l) = (1.96 \pm 0.66) \times \left|\frac{V_{cb}}{0.040}\right|^2 10^{-15} GeV \ , \tag{92}$$

$$\Gamma(B_s \to D_{s1} l\bar{\nu}_l) = (1.08 \pm 0.35) \times \left|\frac{V_{cb}}{0.040}\right|^2 10^{-15} GeV \ , \tag{93}$$

$$\Gamma(B_s \to D_{s2}^* l\bar{\nu}_l) = (1.74 \pm 0.62) \times \left|\frac{V_{cb}}{0.040}\right|^2 10^{-15} GeV \ . \tag{94}$$

Corresponding branching ratios are (using $V_{cb} = 0.040$):

$$BR(B \to D_1 l\bar{\nu}_l) = (0.27 \pm 0.08)\frac{\tau_B}{1.50ps}\% \ , \tag{95}$$

$$BR(B \to D_2^* l\bar{\nu}_l) = (0.45 \pm 0.14)\frac{\tau_B}{1.50ps}\% \ , \tag{96}$$

$$BR(B_s \to D_{s1} l\bar{\nu}_l) = (0.22 \pm 0.07)\frac{\tau_{B_s}}{1.34ps}\% \ , \tag{97}$$

$$BR(B_s \to D_{s2}^* l\bar{\nu}_l) = (0.36 \pm 0.13)\frac{\tau_{B_s}}{1.34ps}\% \ . \tag{98}$$

For comparison with an earlier work, we quote results from [14], where B meson decays into charmed higher resonances were considered:

$$\Gamma(B \to D_1 l\bar{\nu}_l) = 0.36 \times \left|\frac{V_{cb}}{0.040}\right|^2 10^{-15} GeV \ , \tag{99}$$

$$\Gamma(B \to D_2^* l\bar{\nu}_l) = 0.52 \times \left|\frac{V_{cb}}{0.040}\right|^2 10^{-15} GeV \ , \tag{100}$$

$$BR(B \to D_1 l\bar{\nu}_l) = 0.08\frac{\tau_B}{1.50ps}\% \ , \tag{101}$$

$$BR(B \to D_2^* l\bar{\nu}_l) = 0.12\frac{\tau_B}{1.50ps}\% \ . \tag{102}$$

Let us also mention a few earlier calculations of the ξ_E and ξ_F form factors. In [31] these form factors were computed to order $\mathcal{O}((\omega-1)^2)$,

$$\xi_E(\omega) = (1.43 \pm 0.13) - (1.86 \pm 0.28)(\omega - 1) + \mathcal{O}((\omega-1)^2) \ , \tag{103}$$

$$\xi_F(\omega) = (1.14 \pm 0.04) - (2.20 \pm 0.16)(\omega - 1) + \mathcal{O}((\omega-1)^2) \ , \tag{104}$$

where the quoted errors are due to a 12% variation over the scale parameter of the HO wave function. This should be compared with our HO estimates for $\xi_F(1)$ and

$\xi'_F(1)$ given in Tables 5 and 6 (our errors are due to 25% variation of $\beta_S = \beta_P = 0.4$). Assuming that the $E_{\bar{q}}$ value for the $j = \frac{1}{2}$ P wave doublet is the same as the one for the $j = \frac{3}{2}$ P wave doublet[2], our prediction for ξ_E can be obtained using (53) and (54). In particular, using $\xi_F(1) = 1.23$, we find $\xi_E(1) = 1.42$. Note that models based on the Dirac equation can result in ξ_E being larger than ξ_F. In [33] the QCD sum rule calculation yielded $\xi_E(1) = 1.2 \pm 0.7$ (ξ_F was not determined), while a Bethe-Salpeter approach of [34] resulted in $\xi_E(1) = 0.73$ and $\xi_F(1) = 0.76$

Finally, in Figures 8 and 9 we show differential branching ratios $\frac{dBR}{d\omega}$ for the decays $B \to D_1 l \bar{\nu}_l$ and $B \to D_2^* l \bar{\nu}_l$, respectively, obtained from the four different models used in this paper. Differential branching ratios for the corresponding B_s decays are shown in Figures 10 and 11. These calculations assumed the model parameters given in (60), (63), (67) and (70). We also assumed $V_{cb} = 0.040$, $\tau_B = 1.50 \times 10^{-12} s$ and $\tau_{B_s} = 1.34 \times 10^{-12} s$. Differential branching ratios resulting from the one basis state estimates can be obtained using expressions (78) and (88), with parameters given in (74)-(77) and (84)-(87).

7 Conclusion

In this paper we have considered semileptonic B and B_s meson decays into the observed charmed P wave states, in the limit where both b and c quarks are considered heavy. We have estimated the unknown form factors in terms of overlaps of the wave functions describing the final and initial states of the light degrees of freedom. Unlike in previous work [14], our form factor definitions are consistent with the covariant trace formalism of HQET. As a result of this, we find significantly different results

[2]This assumption is valid for the NRQM and the SRQM, which do not distinguish between doublets of the same orbital angular momentum but with different j. However, in the spirit of the one basis state analysis described above, where experimental mass splitting between doublets is used for determination of $E_{\bar{q}}$, $E_{\bar{q}}$'s for the two P wave doublets will be slightly different.

for decay rates and branching ratios for processes $B \to D_1 l\bar{\nu}_l$ and $B \to D_2^* l\bar{\nu}_l$.

In order to examine the sensitivity of our results to the choice of a specific model, we have performed all calculations using several different models. By fixing m_c in the range range from 1.2 GeV to 1.6 GeV, and varying the other model parameters until a good description of the spin-averaged heavy-light spectrum is obtained, we have also examined dependence of our results on the choice of parameters within a specific model. We have also investigated two examples of one basis state calculations. In those cases the uncertainties were estimated from the range of acceptable $E_{\bar{q}}$ values consistent with the experimental data [5] for the decay $B \to D^{(*)} l\bar{\nu}_l$ (as in [32]). This proceedure leads to the conclusion that the choice of parameters within the model introduces errors at the level of (5-30)%. Although six models in all are considered we should emphasize that three (SRQM, DESC, and SEVC), are particularly reliable since they account for the observed D and B spectroscopies in a very satisfactory manner. Between these three models, we find that the predictive accuracy for the unknown form factors is about 30%.

The experimental status for $B \to D_J l\bar{\nu}_l$ is still uncertain. At present three experimental groups [35, 36, 37] have results for these decays but with possible additional non-charmed particle(s) X. These results are given in Table 9 together with our theoretical predictions which assume $BR(D_1 \to D^*\pi) = 67\%$ and $BR(D_2^* \to D^*\pi) = 20\%$. As we can see from Table 9 our predicted branching ratios are consistent with present measurements. In particular, all upper limits are satisfied, and where branching ratios have been determined they are somewhat greater than our predictions (in which there are no additional particles X).

From Tables 5 and 6 we see that the sum of branching ratios into D_1 and D_2^* is about 0.72% (from the three realistic models). By counting spin states we estimate the total P wave meson branching ratio (E, E^*, F, F^*) is about 1.08% (for $V_{cb} = 0.040$ and $\tau_B = 1.5ps$). Thus the P wave states account for about one third of the missing semileptonic B decays.

In this work we have considered only the helicity averaged decay rates. The same Isgur-Wise form factors also appear in the calculation of partial rates into polarized current components and in the angular decay distributions [38, 39]. These angular correlation measurements would provide additional information on the decay dynamics, which would be useful in determining the validity of various theoretical models.

ACKNOWLEDGMENTS

One of us (SV) would like to thank J. F. Beacom for many helpful conversations. This work was supported in part by the U.S. Department of Energy under Contract No. DE-FG02-95ER40896 and in part by the University of Wisconsin Research Committee with funds granted by the Wisconsin Alumni Research Foundation.

References

[1] N. Isgur and M. B. Wise, Phys. Lett. B **232**, 113 (1989); Phys. Lett. B **237**, 527 (1990).

[2] H. Georgi, Phys. Lett. B **240**, 447 (1990).

[3] There are many excellent reviews on the subject of heavy quark symmetry and effective theory. See, for example, H. Georgi, in Proceedings of TASI-91, edt. by R. K. Ellis et al., World Scientific, 1991; N. Isgur and M. B. Wise, in *Heavy Flavors*, edt. by. A. J. Bouras and M. Lindner, World Scientific, 1992; M. Neubert, Phys. Rept. **245**, 259 (1994).

[4] J. Gronberg et al., *Measurement of the branching ratio $B^- \to Xe^-\bar{\nu}_e$ with lepton tags*, report CLEO-CONF-94-6.

[5] B. Barish et al., Phys. Rev. D **51**, 1014 (1995); Y. Kubota et al., *Measurement of the $B(B \to D_0 e^- \bar{\nu}$ using neutrino reconstruction techniques*, report CLEO-CONF-95-10.

[6] H. Georgi, Nucl. Phys. B **348**, 293 (1991).

[7] J. G. Körner and G. A. Schuler, Z. Phys. C **38**, 511 (1988).

[8] A. F. Falk, Phys. Lett. B **378**, 79 (1992).

[9] S. Veseli and M. G. Olsson, *Modelling form factors in HQET*, UW-Madison report MADPH-95-899 (hep-ph/9507425).

[10] A. Ali, T. Ohl, and T. Mannel, Phys. Lett. B **298**, 195 (1993).

[11] L. Montanet et al., Particle Data Group, Phys. Rev. D **50**, 1173 (1994).

[12] M. Neubert, Phys. Lett B **264**, 455 (1991).

[13] M. Sadzikowski and K. Zalewski, Z. Phys. C **59**, 677 (1993).

[14] T. B. Suzuki, T. Ito, S. Sawada, and M. Matsuda, Prog. Theor. Phys. **91**, 757 (1994).

[15] N. Isgur, D. Scora, B. Grinstein, and M. B. Wise, Phys. Rev. D **39**, 799 (1989).

[16] K. Zalewski, Phys. Lett. B **264**, 432 (1991).

[17] E. J. Weniger, J. Math. Phys. **26**, (1985).

[18] A. Duncan, E. Eichten, and H. Thacker, Phys. Lett. B **303**, 109 (1993).

[19] C. Goebel, D. LaCourse, and M. G. Olsson, Phys. Rev. D **41**, 2917 (1990).

[20] M. G. Olsson, S. Veseli, and K. Williams, Phys. Rev. D **51**, 5079 (1995).

[21] V. D. Barger and D. B. Cline, *Phenomenological Theories of High Energy Scattering*, W. A. Benjamin Inc., New York, 1969.

[22] F. Gross, *Relativistic Quantum Mechanics and Field Theory*, John Wiley & Sons, Inc., 1993.

[23] E. E. Salpeter and H. A. Bethe, Phys. Rev. **76**, 1232 (1949).

[24] M. Gell-Mann and F. Low, Phys. Rev. **84**, 350 (1951).

[25] E. E. Salpeter, Phys. Rev. **87**, 328 (1952).

[26] C. Long and D. Robson, Phys. Rev. D **27**, 644 (1983).

[27] G. Hardekopf and J. Sucher, Phys. Rev. A **30**, 703 (1984); Phys. Rev A **31**, 2020 (1985).

[28] Milton S. Plesset, Phys. Rev. **41**, 278 (1932).

[29] J.-F. Lagaë, Phys. Rev. D **45**, 317 (1992).

[30] M. G. Olsson, S. Veseli, and K. Williams, *On the instantaneous Bethe-Salpeter equation*, UW-Madison report, MADPH-95-880 (hep-ph/9503477), to be published in Phys. Rev. D.

[31] A. Wambach, Nucl. Phys. B **434**, 647 (1995).

[32] M. G. Olsson and S. Veseli, Phys. Lett. B. **353**, 96 (1995).

[33] B. Blok and M. Shifman, Phys. Rev. D **47**, 2949 (1993).

[34] Y.-B. Dai, C.-S. Huang, and H.-Y. Jin, Z. Phys. C **60**, 527 (1993).

[35] J. P. Alexander et al., *Semileptonic B meson decay to P wave charm mesons*, report CLEO-CONF-95-30.

[36] D. Buskulic et al., Phys. Lett. B **345**, 103 (1995).

[37] R. Akers et al., report CERN-PPE/95-02.

[38] P. Bialas, J. G. Körner, and K. Zalewski, Z. Phys. C **59**, 117 (1993).

[39] S. Balk, J. G. Körner, G. Thompson, and F. Hussain, Z. Phys. C **59**, 283 (1993).

TABLES

Table 1: Heavy-light spin averaged states. Theoretical results are obtained from the ISGW model [15]. Spin-averaged masses are calculated in the usual way, by taking $\frac{3}{4}$ ($\frac{5}{8}$) of the triplet and $\frac{1}{4}$ ($\frac{3}{8}$) of the singlet mass for the $S(P)$ waves).

State		J^P	$^{2S+1}L_J$	Spin-averaged mass (MeV)	Q. n. j	Q. n. k	Theory (MeV)	Error (MeV)
$c\bar{u}$, $c\bar{d}$ quarks								
$D(1867)$	C	0^-	$^1S_0$	$1S$ (1974)	$\frac{1}{2}$	-1	1931	-43
$D^*(2009)$	C^*	1^-	$^3S_1$					
$D_1(2425)$	F	1^+	$^1P_1/^3P_1$	$1P$ (2446)	$\frac{3}{2}$	-2	2447	1
$D_2^*(2459)$	F^*	2^+	$^3P_2$					
$c\bar{s}$ quarks								
$D_s(1969)$	C	0^-	$^1S_0$	$1S$ (2076)	$\frac{1}{2}$	-1	1982	-94
$D_s^*(2112)$	C^*	1^-	$^3S_1$					
$D_{s1}(2535)$	F	1^+	$^1P_1/^3P_1$	$1P$ (2559)	$\frac{3}{2}$	-2	2473	-86
$D_{s2}^*(2573)$	F^*	2^+	$^3P_2$					
$b\bar{u}$, $b\bar{d}$ quarks								
$B(5279)$	C	0^-	$^1S_0$	$1S$ (5314)	$\frac{1}{2}$	-1	5188	-126
$B^*(5325)$	C^*	1^-	$^3S_1$					
$b\bar{s}$ quarks								
$B_s(5374)$	C	0^-	$^1S_0$	$1S$ (5409)	$\frac{1}{2}$	-1	5216	-193
$B_s^*(5421)$	C^*	1^-	$^3S_1$					

Table 2: Heavy-light spin averaged states. Theoretical results are obtained from the SRQM. Parameters of the model are given in (63). Spin-averaged masses are calculated in the usual way, by taking $\frac{3}{4}$ ($\frac{5}{8}$) of the triplet and $\frac{1}{4}$ ($\frac{3}{8}$) of the singlet mass for the $S(P)$ waves).

State		Spectroscopic label J^P	$^{2S+1}L_J$	Spin-averaged mass (MeV)	Q. n. j	k	Theory (MeV)	Error (MeV)
$c\bar{u}$, $c\bar{d}$ quarks								
$D(1867)$	C	0^-	$^1S_0$	$1S$ (1974)	$\frac{1}{2}$	-1	1974	0
$D^*(2009)$	C^*	1^-	$^3S_1$					
$D_1(2425)$	F	1^+	$^1P_1/^3P_1$	$1P$ (2446)	$\frac{3}{2}$	-2	2449	3
$D_2^*(2459)$	F^*	2^+	$^3P_2$					
$c\bar{s}$ quarks								
$D_s(1969)$	C	0^-	$^1S_0$	$1S$ (2076)	$\frac{1}{2}$	-1	2075	-1
$D_s^*(2112)$	C^*	1^-	$^3S_1$					
$D_{s1}(2535)$	F	1^+	$^1P_1/^3P_1$	$1P$ (2559)	$\frac{3}{2}$	-2	2557	-2
$D_{s2}^*(2573)$	F^*	2^+	$^3P_2$					
$b\bar{u}$, $b\bar{d}$ quarks								
$B(5279)$	C	0^-	$^1S_0$	$1S$ (5314)	$\frac{1}{2}$	-1	5311	-3
$B^*(5325)$	C^*	1^-	$^3S_1$					
$b\bar{s}$ quarks								
$B_s(5374)$	C	0^-	$^1S_0$	$1S$ (5409)	$\frac{1}{2}$	-1	5412	3
$B_s^*(5421)$	C^*	1^-	$^3S_1$					

Table 3: Heavy-light spin averaged states. Theoretical results are obtained from the Dirac equation with scalar confinement. Parameters of the model are given in (67). Spin-averaged masses are calculated in the usual way, by taking $\frac{3}{4}$ ($\frac{5}{8}$) of the triplet and $\frac{1}{4}$ ($\frac{3}{8}$) of the singlet mass for the $S(P)$ waves).

State		J^P	$^{2S+1}L_J$	Spin-averaged mass (MeV)	Q. n. j	Q. n. k	Theory (MeV)	Error (MeV)
$c\bar{u}$, $c\bar{d}$ quarks								
$D(1867)$	C	0^-	$^1S_0$	$1S$ (1974)	$\frac{1}{2}$	-1	1977	3
$D^*(2009)$	C^*	1^-	$^3S_1$					
$D_1(2425)$	F	1^+	$^1P_1/^3P_1$	$1P$ (2446)	$\frac{3}{2}$	-2	2444	-2
$D_2^*(2459)$	F^*	2^+	$^3P_2$					
$c\bar{s}$ quarks								
$D_s(1969)$	C	0^-	$^1S_0$	$1S$ (2076)	$\frac{1}{2}$	-1	2074	-2
$D_s^*(2112)$	C^*	1^-	$^3S_1$					
$D_{s1}(2535)$	F	1^+	$^1P_1/^3P_1$	$1P$ (2559)	$\frac{3}{2}$	-2	2560	1
$D_{s2}^*(2573)$	F^*	2^+	$^3P_2$					
$b\bar{u}$, $b\bar{d}$ quarks								
$B(5279)$	C	0^-	$^1S_0$	$1S$ (5314)	$\frac{1}{2}$	-1	5313	-1
$B^*(5325)$	C^*	1^-	$^3S_1$					
$b\bar{s}$ quarks								
$B_s(5374)$	C	0^-	$^1S_0$	$1S$ (5409)	$\frac{1}{2}$	-1	5410	1
$B_s^*(5421)$	C^*	1^-	$^3S_1$					

Table 4: Heavy-light spin averaged states. Theoretical results are obtained from the Salpeter equation with vector confinement (in the heavy-light limit). Parameters of the model are given in (70). Spin-averaged masses are calculated in the usual way, by taking $\frac{3}{4}$ ($\frac{5}{8}$) of the triplet and $\frac{1}{4}$ ($\frac{3}{8}$) of the singlet mass for the $S(P)$ waves).

State		J^P	$^{2S+1}L_J$	Spin-averaged mass (MeV)	Q. n. j	Q. n. k	Theory (MeV)	Error (MeV)
$c\bar{u}$, $c\bar{d}$ quarks								
$D(1867)$	C	0^-	$^1S_0$	$1S$ (1974)	$\frac{1}{2}$	-1	1980	6
$D^*(2009)$	C^*	1^-	$^3S_1$					
$D_1(2425)$	F	1^+	$^1P_1/^3P_1$	$1P$ (2446)	$\frac{3}{2}$	-2	2439	-7
$D_2^*(2459)$	F^*	2^+	$^3P_2$					
$c\bar{s}$ quarks								
$D_s(1969)$	C	0^-	$^1S_0$	$1S$ (2076)	$\frac{1}{2}$	-1	2072	-4
$D_s^*(2112)$	C^*	1^-	$^3S_1$					
$D_{s1}(2535)$	F	1^+	$^1P_1/^3P_1$	$1P$ (2559)	$\frac{3}{2}$	-2	2564	5
$D_{s2}^*(2573)$	F^*	2^+	$^3P_2$					
$b\bar{u}$, $b\bar{d}$ quarks								
$B(5279)$	C	0^-	$^1S_0$	$1S$ (5314)	$\frac{1}{2}$	-1	5316	2
$B^*(5325)$	C^*	1^-	$^3S_1$					
$b\bar{s}$ quarks								
$B_s(5374)$	C	0^-	$^1S_0$	$1S$ (5409)	$\frac{1}{2}$	-1	5407	-2
$B_s^*(5421)$	C^*	1^-	$^3S_1$					

Table 5: Results for the decay $B \to D_1 l \bar{\nu}_l$ obtained from four different models and two one basis state estimates. Errors for the SRQM, DESC, and SEVC, are due to variation of m_c in the range from 1.2 GeV to 1.6 GeV. Errors for the PC and HO estimates are due to variation of $\beta_S = \beta_P$ in the range from 0.3 GeV to 0.5 GeV. For the reference values of the B meson lifetime we take [11] $\tau_B^{ref} = 1.50 \times 10^{-12} s$, and for the reference value of V_{cb} we take 0.040.

Model	$\xi_F(1)$	$\xi'_F(1)$	$\Gamma\ [\left\lvert\frac{V_{cb}}{0.040}\right\rvert^2 10^{-15} GeV]$	$BR\ [\frac{\tau_B}{\tau_B^{ref}}\%]$
ISGW	0.60	-0.89	0.73	0.17
SRQM	0.84 ± 0.19	-2.04 ± 0.77	1.01 ± 0.34	0.23 ± 0.08
DESC	0.79 ± 0.14	-1.45 ± 0.44	1.07 ± 0.24	0.25 ± 0.06
SEVC	1.18 ± 0.19	-4.04 ± 1.31	1.41 ± 0.22	0.32 ± 0.05
PC	1.42 ± 0.26	-6.23 ± 2.70	1.61 ± 0.06	0.37 ± 0.02
HO	1.23 ± 0.21	-3.23 ± 1.18	1.94 ± 0.28	0.44 ± 0.06

Table 6: Results for the decay $B \to D_2^* l \bar{\nu}_l$ obtained from four different models and two one basis state estimates. Errors for the SRQM, DESC, and SEVC, are due to variation of m_c in the range from 1.2 GeV to 1.6 GeV. Errors for the PC and HO estimates are due to variation of $\beta_S = \beta_P$ in the range from 0.3 GeV to 0.5 GeV. We take [11] $\tau_B^{ref} = 1.50 \times 10^{-12} s$ and $V_{cb} = 0.040$.

Model	$\xi_F(1)$	$\xi'_F(1)$	$\Gamma\ [\left\lvert\frac{V_{cb}}{0.040}\right\rvert^2 10^{-15} GeV]$	$BR\ [\frac{\tau_B}{\tau_B^{ref}}\%]$
ISGW	0.60	-0.89	1.14	0.26
SRQM	0.84 ± 0.19	-2.04 ± 0.77	1.69 ± 0.56	0.38 ± 0.13
DESC	0.79 ± 0.14	-1.45 ± 0.44	1.77 ± 0.45	0.41 ± 0.11
SEVC	1.18 ± 0.19	-4.04 ± 1.31	2.41 ± 0.41	0.55 ± 0.10
PC	1.42 ± 0.26	-6.23 ± 2.70	2.80 ± 0.18	0.64 ± 0.04
HO	1.23 ± 0.21	-3.23 ± 1.18	3.23 ± 0.55	0.74 ± 0.13

Table 7: Results for the decay $B_s \to D_{s1} l \bar{\nu}_l$ obtained from four different models and two one basis state estimates. Errors for the SRQM, DESC, and SEVC, are due to variation of m_c in the range from 1.2 GeV to 1.6 GeV. Errors for the PC and HO estimates are due to variation of $\beta_S = \beta_P$ in the range from 0.3 GeV to 0.5 GeV. We take [11] $\tau_{B_s}^{ref} = 1.34 \times 10^{-12} s$ and $V_{cb} = 0.040$.

Model	$\xi_F(1)$	$\xi'_F(1)$	$\Gamma\ [\left\lvert\frac{V_{cb}}{0.040}\right\rvert^2 10^{-15} GeV]$	$BR\ [\frac{\tau_{B_s}}{\tau_{B_s}^{ref}}\%]$
ISGW	0.51	-0.71	0.53	0.11
SRQM	0.84 ± 0.21	-2.09 ± 0.81	0.98 ± 0.34	0.20 ± 0.07
DESC	0.82 ± 0.14	-1.59 ± 0.47	1.10 ± 0.27	0.23 ± 0.06
SEVC	0.97 ± 0.22	-2.75 ± 1.04	1.15 ± 0.34	0.24 ± 0.07
PC	1.70 ± 0.34	-9.98 ± 4.73	1.57 ± 0.11	0.32 ± 0.02
HO	1.42 ± 0.26	-4.59 ± 1.87	2.08 ± 0.21	0.43 ± 0.05

Table 8: Results for the decay $B \to D_{s2}^* l \bar{\nu}_l$ obtained from four different models and two one basis state estimates. Errors for the SRQM, DESC, and SEVC, are due to variation of m_c in the range from 1.2 GeV to 1.6 GeV. Errors for the PC and HO estimates are due to variation of $\beta_S = \beta_P$ in the range from 0.3 GeV to 0.5 GeV. For the reference values of the We take [11] $\tau_{B_s}^{ref} = 1.34 \times 10^{-12} s$ and $V_{cb} = 0.040$.

Model	$\xi_F(1)$	$\xi'_F(1)$	$\Gamma\ [\left\lvert\frac{V_{cb}}{0.040}\right\rvert^2 10^{-15} GeV]$	$BR\ [\frac{\tau_{B_s}}{\tau_{B_s}^{ref}}\%]$
ISGW	0.51	-0.71	0.81	0.17
SRQM	0.84 ± 0.21	-2.09 ± 0.81	1.58 ± 0.57	0.32 ± 0.12
DESC	0.82 ± 0.14	-1.59 ± 0.47	1.75 ± 0.45	0.36 ± 0.09
SEVC	0.97 ± 0.22	-2.75 ± 1.04	1.90 ± 0.60	0.39 ± 0.12
PC	1.70 ± 0.34	-9.98 ± 4.73	2.90 ± 0.08	0.59 ± 0.02
HO	1.42 ± 0.26	-4.59 ± 1.87	3.52 ± 0.48	0.72 ± 0.10

Table 9: A summary of experimental results for $B \to D_J X e^- \bar{\nu}$, where X is a possible non-charmed hadron. Our theoretical predictions are obtained from (95) and (96) for the pure semileptonic decays $B \to D_J e^- \bar{\nu}$, assuming $BR(D_1^0 \to D^{*+}\pi^-) = 67\%$ and $BR(D_2^{*0} \to D^{*+}\pi^-) = 20\%$.

Decay Mode	CLEO [35] [%]	ALEPH [36] [%]	OPAL [37] [%]	This work [%]
$BR(B \to D_1^0 X e^- \bar{\nu})$ $\times BR(D_1^0 \to D^{*+}\pi^-)$	< 0.67 (90% c.l.)	0.51 ± 0.17	1.36 ± 0.46	0.18 ± 0.05
$BR(B \to D_2^{*0} X e^- \bar{\nu})$ $\times BR(D_2^{*0} \to D^{*+}\pi^-)$	< 0.79 (90% c.l.)	< 0.20 (95% c.l.)	0.18 ± 0.08	0.09 ± 0.03

FIGURES

Figure 1: ξ_F for the semileptonic decays $B \to D_1, D_2^*$, obtained from the ISGW model [15]. The full line shows our prediction (VO), obtained from (47), while the dashed line is AOM prediction obtained from (35), which is used in [10, 14].

Figure 2: ξ_F for the semileptonic decays $B_s \to D_{s1}, D_{s2}^*$, obtained from the ISGW model [15]. The full line shows our prediction (VO), obtained from (47), while the dashed line is AOM prediction obtained from (35), which is used in [10, 14].

Figure 3: ξ_F for the semileptonic decays $B \to D_1, D_2^*$, obtained from the SRQM (dotted line), DESC (dashed line), and SEVC (full line). Model parameters are given in (63), (67) and (70), respectively.

Figure 4: ξ_F for the semileptonic decays $B_s \to D_{s1}, D_{s2}^*$, obtained from the SRQM (dotted line), DESC (dashed line), and SEVC (full line). Model parameters are given in (63), (67) and (70), respectively.

Figure 5: Comparison of the lattice data with the $1S$ pseudo-Coulombic (full line) and harmonic oscillator (dashed line) wave function. For both wave functions we used $\beta_S = 0.40\ GeV$.

Figure 6: ξ_F for the semileptonic decays $B \to D_1, D_2^*$, obtained from one PC basis state (full line), and from one HO state (dashed line). In both cases we used $\beta_S = \beta_P = 0.40\ GeV$. In the PC case we used $E_{\bar{q}} = 0.320\ GeV$ ((B, B^*) doublet) and $E_{\bar{q}} = 0.792\ GeV$ ((D_1, D_2^*) doublet), and in the HO case $E_{\bar{q}} = 0.444\ GeV$ ((B, B^*) doublet) and $E_{\bar{q}} = 0.916\ GeV$ ((D_1, D_2^*) doublet).

Figure 7: ξ_F for the semileptonic decays $B_s \to D_{s1}, D^*_{s2}$, obtained from one PC basis state (full line), and from one HO state (dashed line). In both cases we used $\beta_S = \beta_P = 0.40\ GeV$. In the PC case we used $E_{\bar{q}} = 0.415\ GeV$ ((B_s, B^*_s) doublet) and $E_{\bar{q}} = 0.905\ GeV$ ((D_{s1}, D^*_{s2}) doublet), and in the HO case $E_{\bar{q}} = 0.539\ GeV$ ((B_s, B^*_s) doublet) and $E_{\bar{q}} = 1.029\ GeV$ ((D_{s1}, D^*_{s2}) doublet).

Figure 8: Differential branching ratio $\frac{dBR}{d\omega}$ for the process $B \to D_1 l \bar{\nu}_l$ $(C \to F)$ obtained from the four different models, with parameters given in (60) (ISGW), (63) (SRQM), (67) (DESC), and (70) (SEVC). For this calculation we used $V_{cb} = 0.040$ and $\tau_B = 1.50 \times 10^{-12} s$. The kinematic limit for this decay is $\omega_{max} = 1.318$.

Figure 9: Differential branching ratio $\frac{dBR}{d\omega}$ for the process $B \to D^*_2 l \bar{\nu}_l$ $(C \to F^*)$ obtained from the four different models, with parameters given in (60) (ISGW), (63) (SRQM), (67) (DESC), and (70) (SEVC). For this calculation we used $V_{cb} = 0.040$ and $\tau_B = 1.50 \times 10^{-12} s$. The kinematic limit for this decay is $\omega_{max} = 1.306$.

Figure 10: Differential branching ratio $\frac{dBR}{d\omega}$ for the process $B_s \to D_{s1} l \bar{\nu}_l$ $(C \to F)$ obtained from the four different models, with parameters given in (60) (ISGW), (63) (SRQM), (67) (DESC), and (70) (SEVC). For this calculation we used $V_{cb} = 0.040$ and $\tau_{B_s} = 1.34 \times 10^{-12} s$. The kinematic limit for this decay is $\omega_{max} = 1.296$.

Figure 11: Differential branching ratio $\frac{dBR}{d\omega}$ for the process $B_s \to D^*_{s2} l \bar{\nu}_l$ $(C \to F^*)$ obtained from the four different models, with parameters given in (60) (ISGW), (63) (SRQM), (67) (DESC), and (70) (SEVC). For this calculation we used $V_{cb} = 0.040$ and $\tau_{B_s} = 1.34 \times 10^{-12} s$. The kinematic limit for this decay is $\omega_{max} = 1.284$.

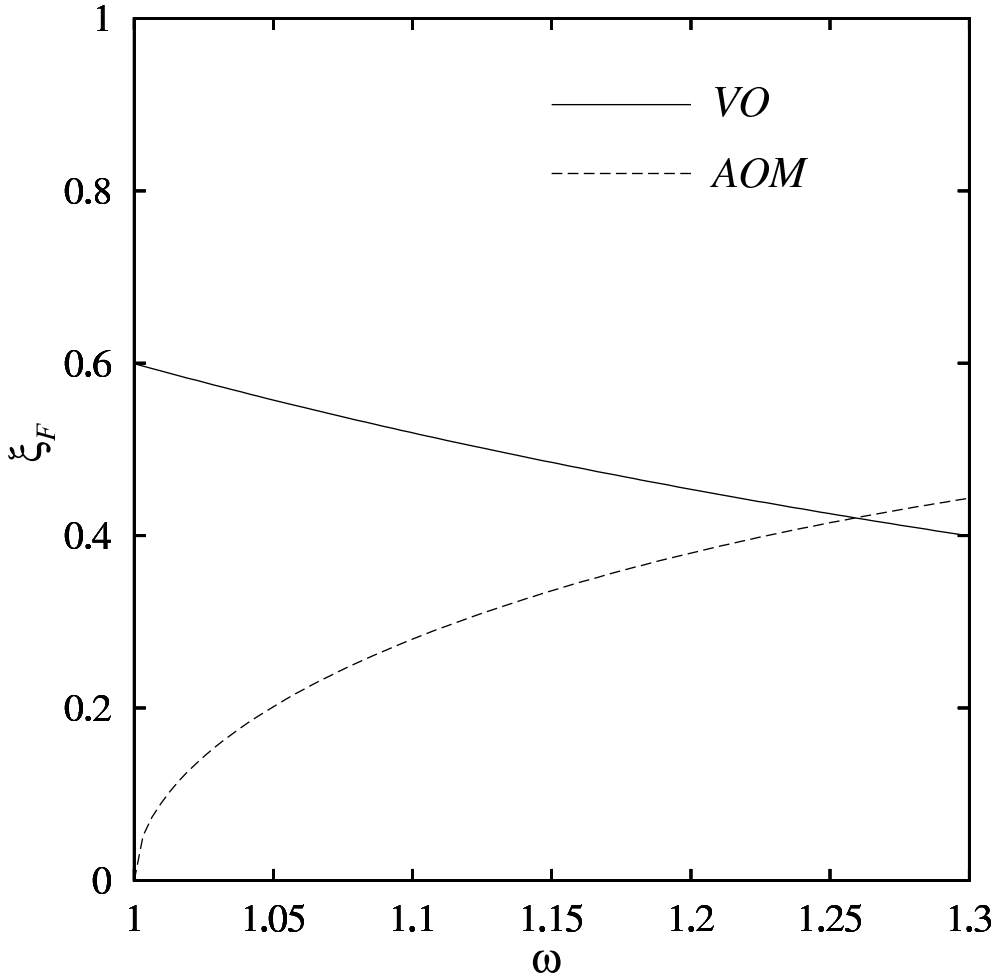

Figure 1

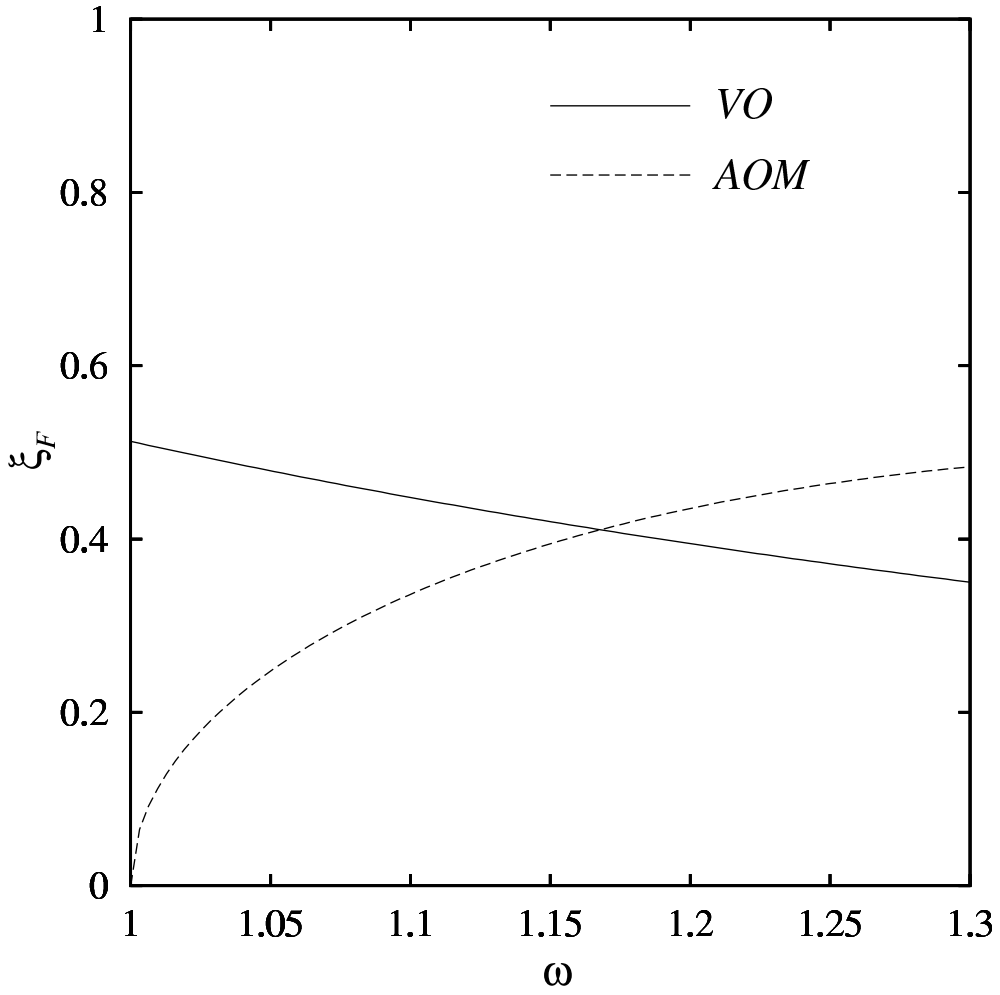

Figure 2

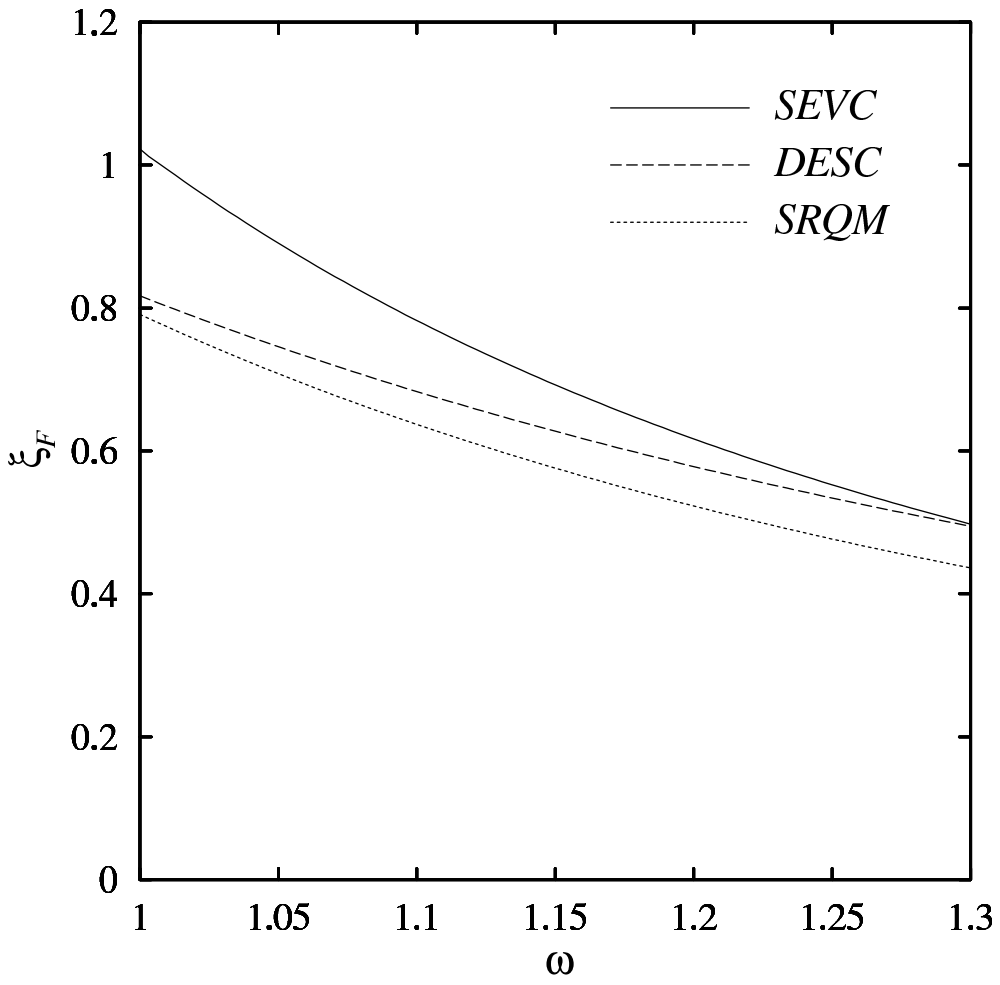

Figure 3

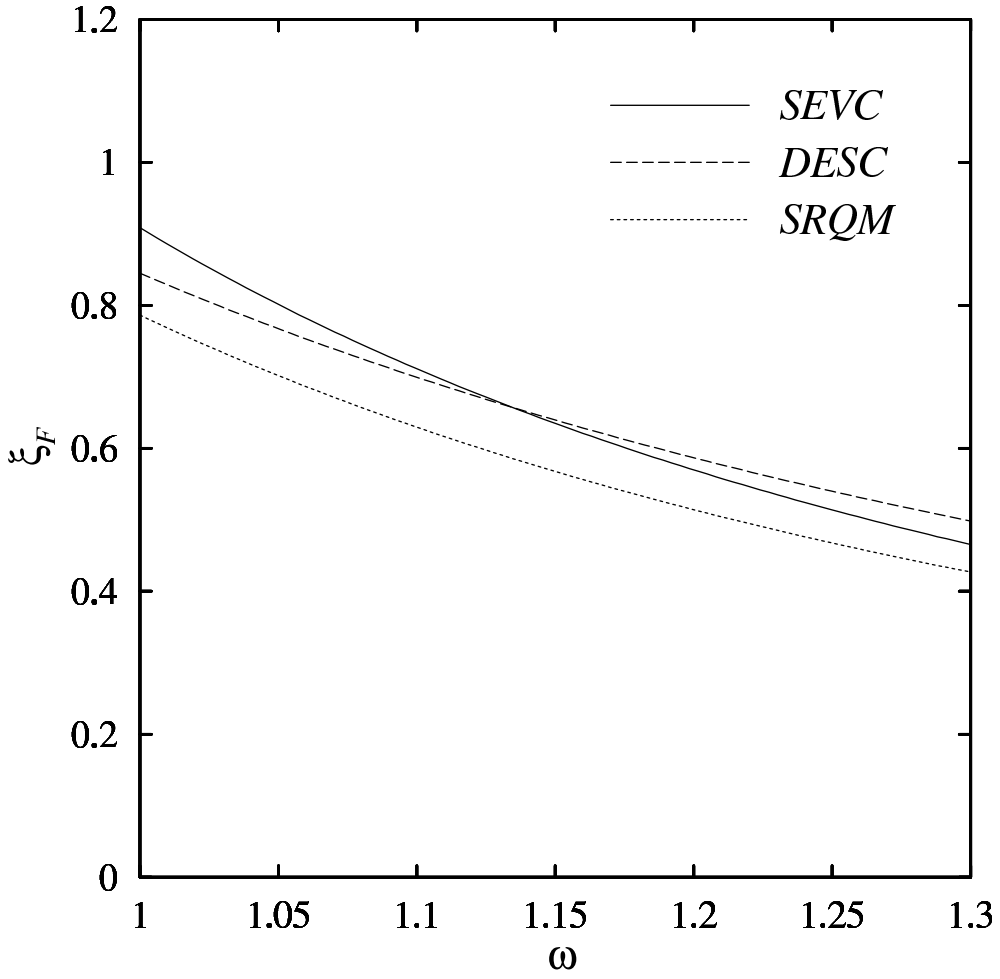

Figure 4

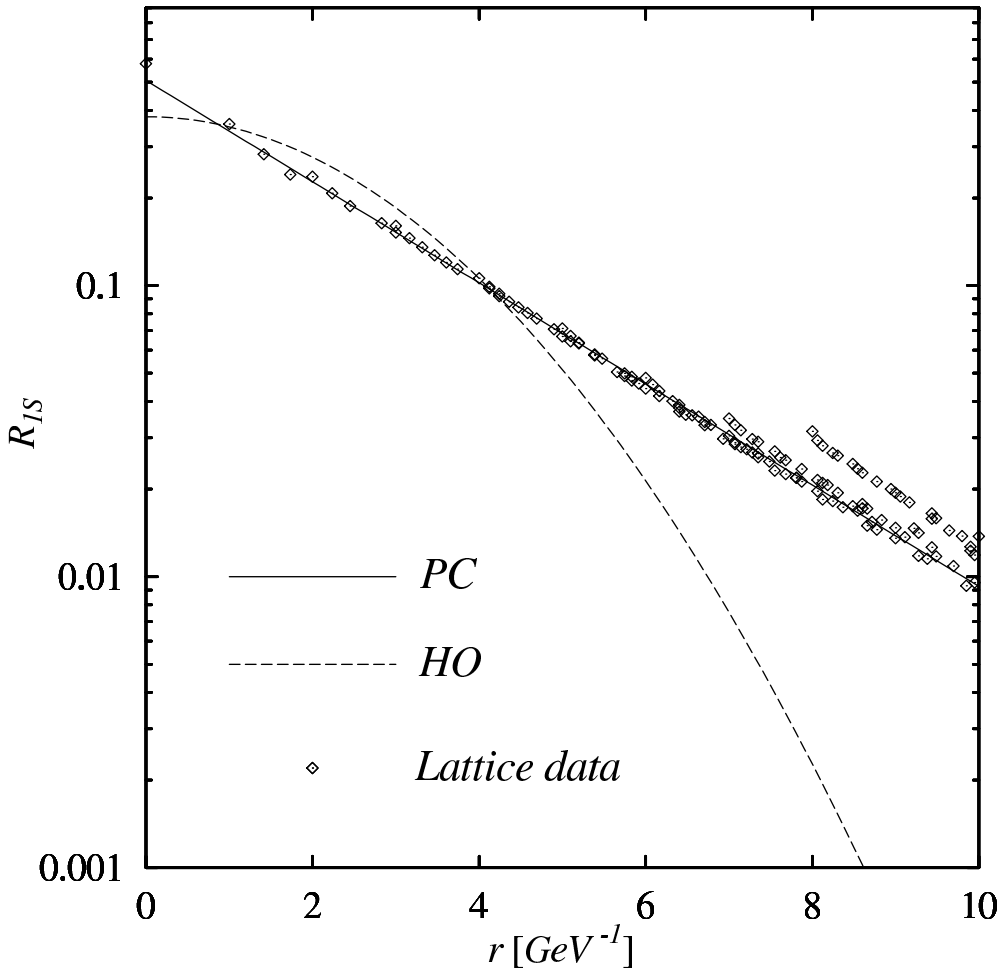

Figure 5

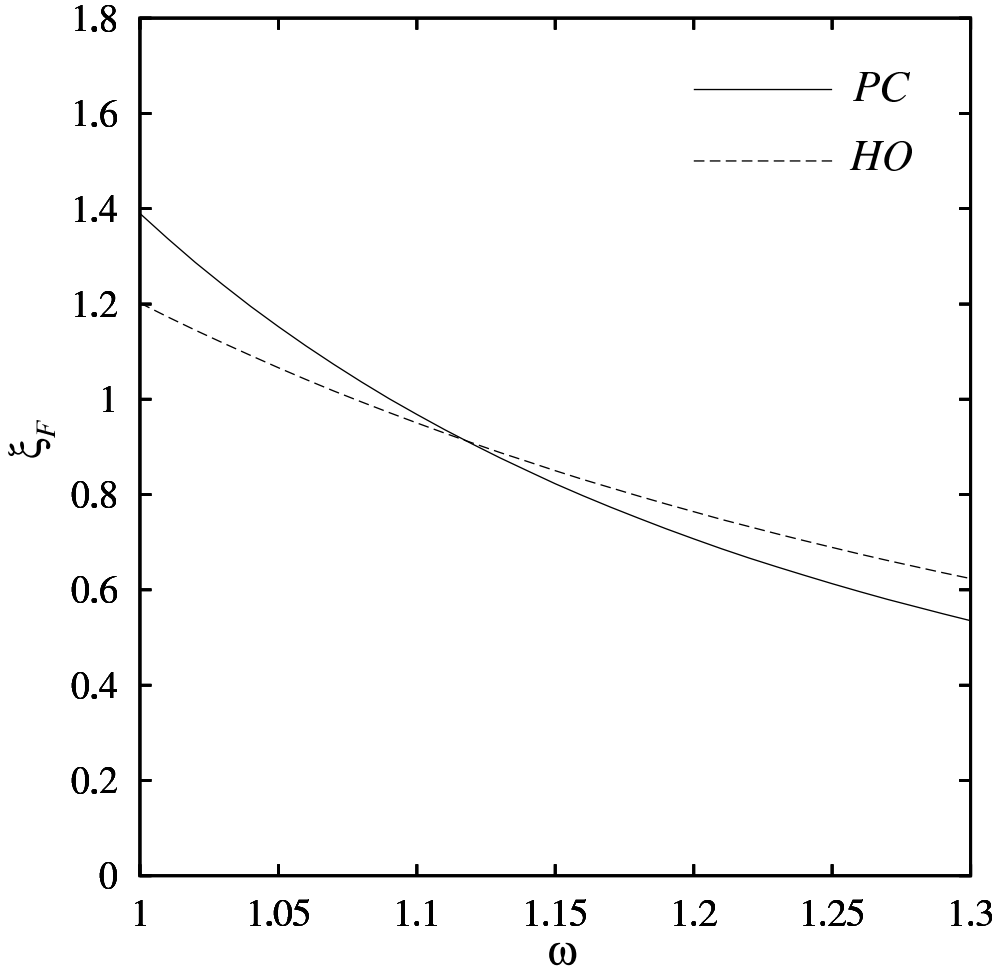

Figure 6

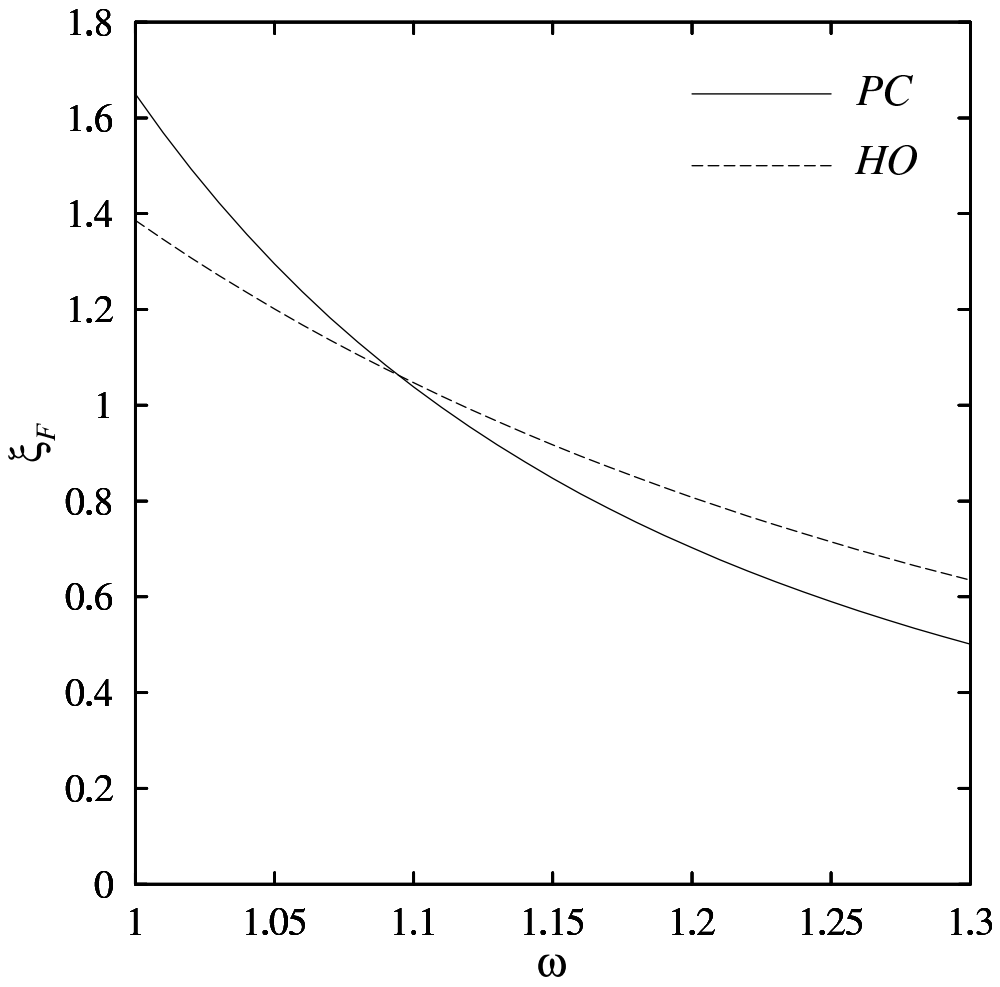

Figure 7

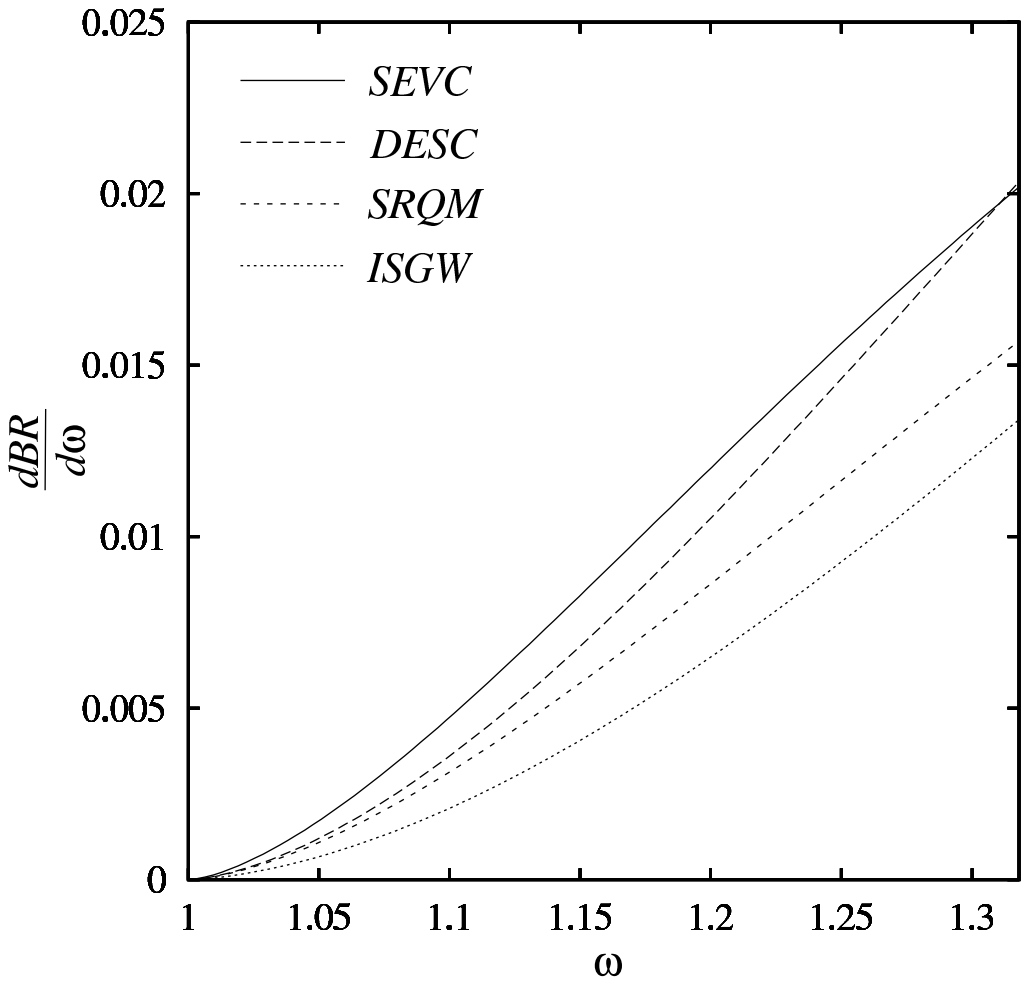
0.025
0.02
0.015
0.01
0.005
0
1
1.05
1.1
1.15
1.2
1.25
1.3
ω
$\frac{dBR}{d\omega}$
SEVC
DESC
SRQM
ISGW

Figure 8

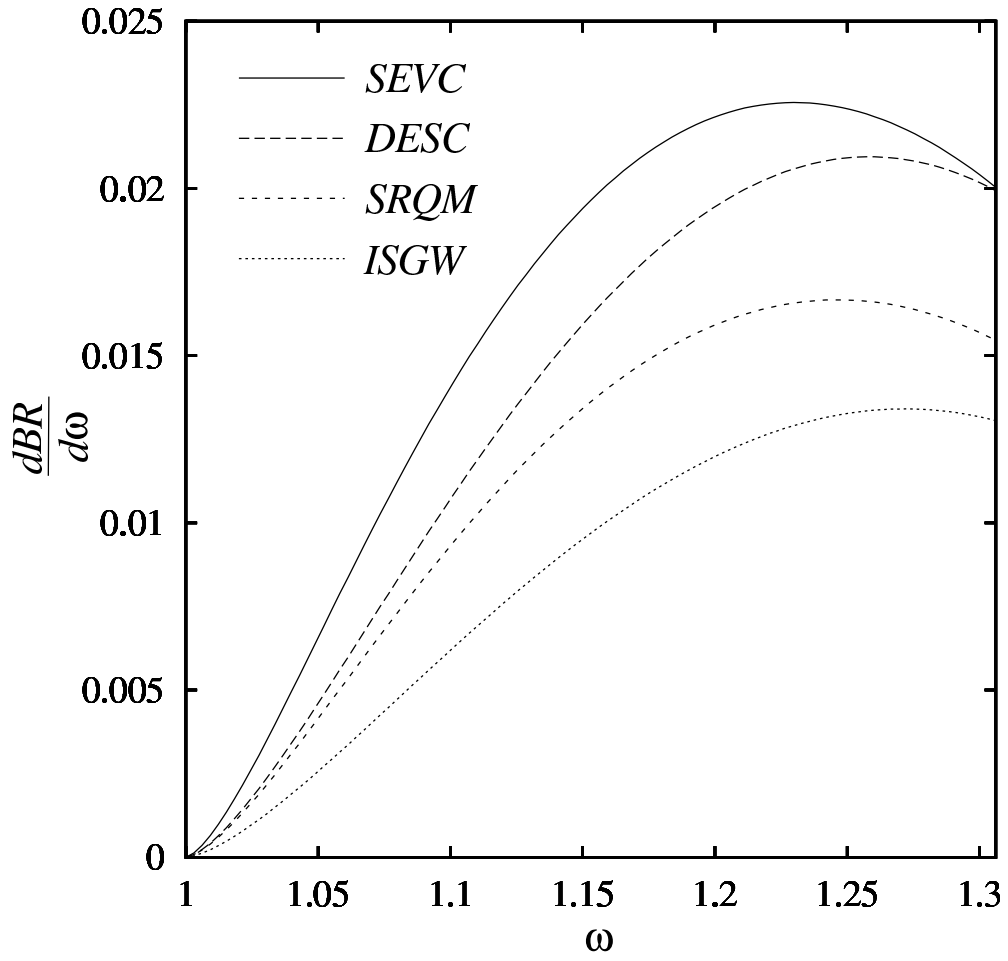
0.025
0.02
0.015
0.01
0.005
0
1
1.05
1.1
1.15
1.2
1.25
1.3
ω
$\frac{dBR}{d\omega}$
SEVC
DESC
SRQM
ISGW

Figure 9

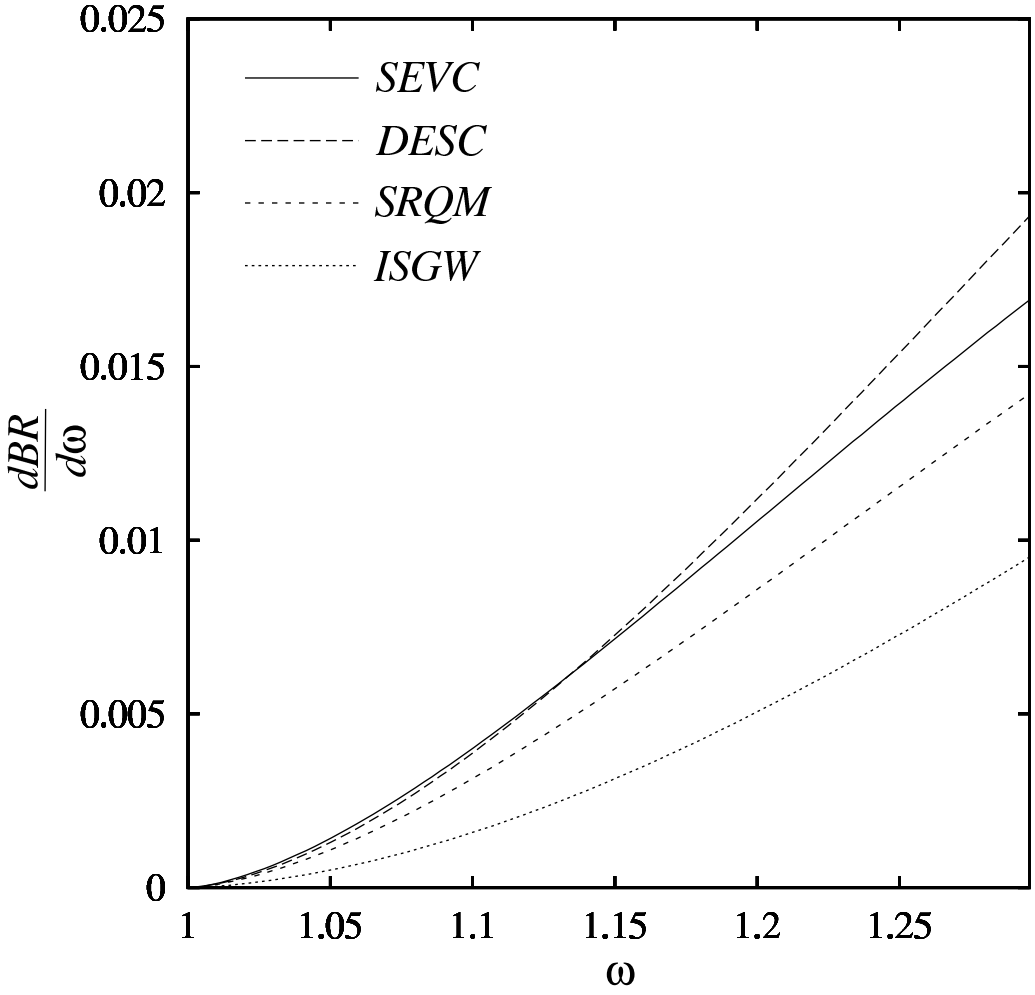
0.025
0.02
0.015
0.01
0.005
0
1
1.05
1.1
1.15
1.2
1.25
ω
dBR/dω
SEVC
DESC
SRQM
ISGW

Figure 10

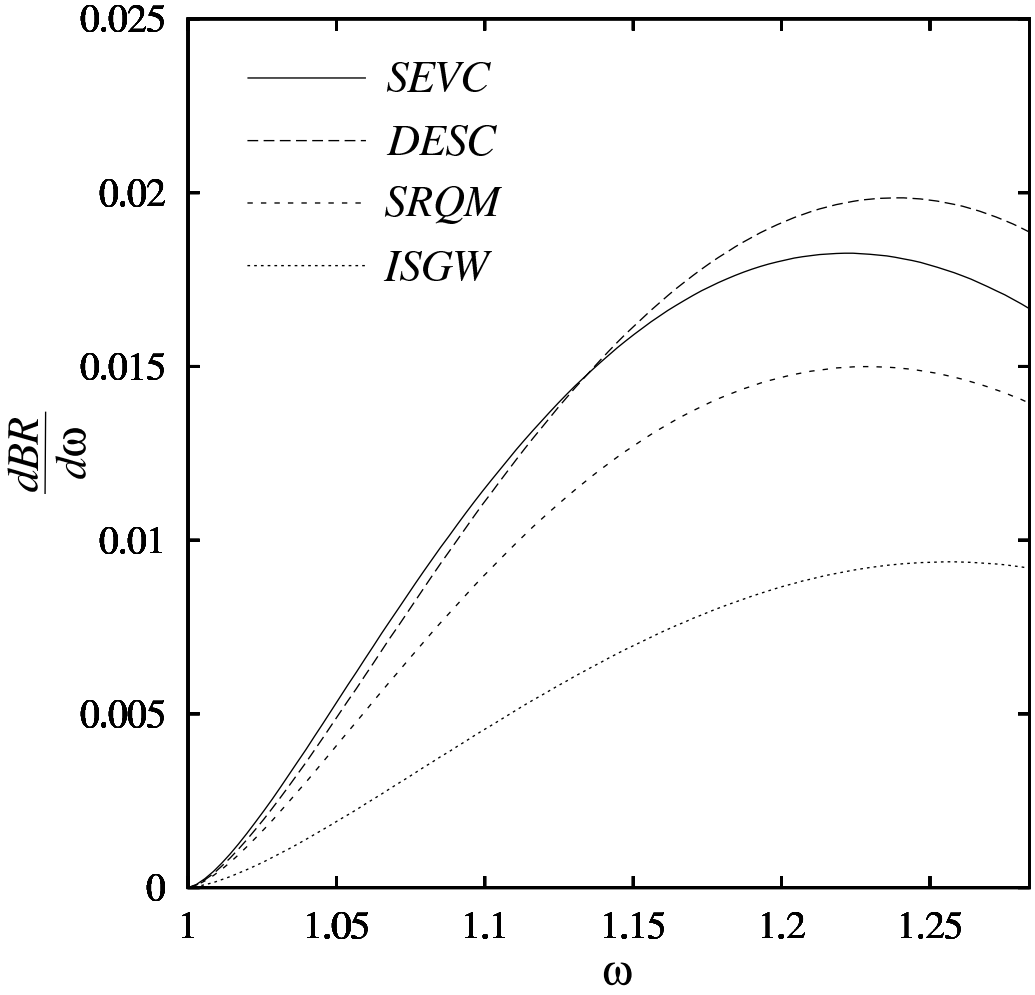
0.025
0.02
0.015
0.01
0.005
0
1
1.05
1.1
1.15
1.2
1.25
ω
$\frac{dBR}{d\omega}$
SEVC
DESC
SRQM
ISGW

Figure 11